Hindawi Publishing Corporation
Interdisciplinary Perspectives on Infectious Diseases
Volume 2010, Article ID 109239, 28 pages
doi:10.1155/2010/109239

Review Article

A Mechanism of Virus-Induced Demyelination

Jayasri Das Sarma

Department of Biological Sciences, Indian Institute of Science Education and Research-Kolkata, Mohanpur Campus, PO: BCKV Campus Main Office, Mohanpur, Nadia, West Bengal 741252, India

Correspondence should be addressed to Jayasri Das Sarma, dassarmaj@iiserkol.ac.in

Received 8 January 2010; Accepted 20 March 2010

Academic Editor: Marylou V. Solbrig

Myelin forms an insulating sheath surrounding axons in the central and peripheral nervous systems and is essential for rapid propagation of neuronal action potentials. Demyelination is an acquired disorder in which normally formed myelin degenerates, exposing axons to the extracellular environment. The result is dysfunction of normal neuron-to-neuron communication and in many cases, varying degrees of axonal degeneration. Numerous central nervous system demyelinating disorders exist, including multiple sclerosis. Although demyelination is the major manifestation of most of the demyelinating diseases, recent studies have clearly documented concomitant axonal loss to varying degrees resulting in long-term disability. Axonal injury may occur secondary to myelin damage (outside-in model) or myelin damage may occur secondary to axonal injury (inside-out model). Viral induced demyelination models, has provided unique imminent into the cellular mechanisms of myelin destruction. They illustrate mechanisms of viral persistence, including latent infections, virus reactivation and viral-induced tissue damage. These studies have also provided excellent paradigms to study the interactions between the immune system and the central nervous system (CNS). In this review we will discuss potential cellular and molecular mechanism of central nervous system axonal loss and demyelination in a viral induced mouse model of multiple sclerosis.

1. Introduction

Demyelination is the process by which axons lose their normal insulating myelin. Several central nervous system demyelinating disorders have been described in humans including multiple sclerosis, neuromyelitis optica (Devic's disease), acute disseminated encephalomyelitis, and osmotic demyelination (central pontine myelinolysis, extrapontine myelinolysis).

Multiple sclerosis (MS) is a chronic, progressive, or relapsing and remitting demyelinating disorder that affects the central nervous system (CNS) specifically and ranks as a major cause of nervous system disability in young adults aged 20 to 45 [1–3]. It has long been hypothesized that oligodendrocytes (OLGs) and/or the myelin sheath are the target of immune system-mediated destruction in MS. Recent studies have demonstrated that axonal damage [4, 5] also occurs and is likely to be a major component of long-term disability observed in MS. The etiology of MS is not very clearly known but the process of demyelination is believed to involve a Tcell-mediated phenomenon that may be triggered by one or more viral infections. Clinical studies show that infectious agents encountered during adolescence prime the diseases, which appear clinically later in the adult after a variable period of quiescence [6, 7]. Despite numerous attempts, a particular responsible virus has not been identified. Our research has focused on understanding the mechanisms of demyelination. We use the mouse hepatitis virus (MHV) model of murine demyelination in order to dissect the inflammatory and molecular mechanisms of viral-induced demyelination.

2. Infectious Etiology of Multiple Sclerosis

The most important evidence that MS might be infectious is based on the fact that the brain and cerebrospinal fluid (CSF) of more than 90% MS patients contain increased amounts of IgG, manifest as oligoclonal bands (OGBs) [8]. There are other but not many CNS disorders in which increased amounts of IgG and OGBs are found. All those diseases are inflammatory, and most are infectious. Furthermore, when the specificity of the increased IgG and OGBs in

those diseases was studied, the IgG in every condition was shown to be antibody directed against the agent that caused disease. For example, the oligoclonal IgG found in subacute sclerosing panencephalitis (SSPE) brain and CSF is directed against measles virus [9] not herpes simplex virus or mumps virus; in cryptococcal meningitis, the IgG is directed against cryptococcus and not another fungus such as candida [10]. These findings provide a rationale for the notion that the oligoclonal IgG in MS brain and CSF is antibody directed against the agent that causes disease.

Moreover, a number of studies have documented viruses as triggers for MS. The fact that viruses are associated with multifocal leukoencephalopathy (PML), SSPE, and postinfectious encephalitis explains the continued interest in viruses as triggers for MS [11, 12]. Studies in herpes virus have been quite extensive, especially in human herpes virus 6 (HHV-6) [13–15] and Epstein-Barr virus (EBV) [16, 17]. Herpes viruses are of particular interest because of their neurotropic, ubiquitous nature and their tendency to produce latent, recurrent infections.

However, there are no studies to date that clearly demonstrate the underlying pathophysiology, correlating the trigger of viral infection with induction of the demyelination process. One key to a better insight into the molecular and cellular mechanisms of MS lies in the development of a reliable animal model. Towards this goal several experimental animal models have been developed to study the mechanisms of virus-induced demyelination.

3. Animal Model for Viral- Induced Demyelinating Diseases

Mouse model studies using Theiler's murine encephalomyelitis virus (TMEV) [18, 19] infection and neurotropic strains of Mouse hepatitis virus (MHV) infection have given useful information on putative MS mechanisms [20–23]. In virus-induced demyelination, infection is a necessary prerequisite for demyelination, and the cause/effect relationship makes this model an attractive platform for exploring the etiology and pathogenesis of demyelinating diseases. Chronic viral-induced dem-yelination is associated with viral persistence [24, 25] and concomitant enhancement of major histocompatibility complex class I antigens [26–30]. These features parallel many of the pathologic findings seen in MS, in contrast to monophasic viral or postviral human demyelinating diseases such as acute disseminated encephalomyelitis (ADEM) [31] and PML [32].

4. TMEV- Induced Demyelination Versus MHV-Induced Demyelination

Infection of susceptible strains of mice with some strains of TMEV or MHV causes biphasic disease of the CNS, consisting of early acute disease and late chronic demyelinating disease that appears 30 to 40 days post infection (p.i) [33]. As early as 30 days p.i, infected mice develop late chronic demyelinating disease with extensive demyelinating lesions of the white matter and cell infiltrates in the spinal cord, consisting primarily of CD4+ T cells and CD8+ T cells, some monocots/macrophages, and a few B cells and plasma cells. In general, viral infection causes damage to the nervous system by two mechanisms: direct infection of neural cells and immune-mediated tissue injury (immunopathology).

Virtually all types of immune response have been proposed to play important roles in the pathogenesis of TMEV-induced viral clearance and demyelination. It has been proposed that demyelination is caused by an immune-mediated mechanism, in which CD4+ Th1 cells mediate a delayed type of hypersensitivity response with epitope spreading [34]. TMEV-induced CD8+ T cells have been suggested to function as autoreactive cytotoxic cells or regulatory cells [35]. Antibody against TMEV cross-reacts with galactocerebroside, and passive transfer of anti-TMEV antibody can augment demyelination in experimental allergic encephalomyelitis (EAE) [36]. Intracerebral inoculation with a TMEV-infected macrophage cell line induces acute focal demyelination [37], and depletion of macrophages ameliorates TMEV-induced demyelination [38].

Evidence from highly neurovirulent *JHM* strains of MHV suggests that MHV-induced demyelination is also primarily immune mediated [39, 40]. Demyelination can be completely eliminated in JHM-infected, RAG $-/-$ mice that lack functional T and B cells, and this process can be reversed upon transfer of splenocytes from immunocompetent mice [41]. It has also been shown by depletion and transfer studies in the JHM model that either CD4+ or CD8+ T cells can induce demyelination.

However, MHV-A59-induced demyelination has been shown to develop in the absence of B and T cells [42]. Furthermore, depletion of CD4+ or CD8+ T cells after the acute stage of infection does not reduce demyelination [43]. Thus, different related strains of MHV may induce demyelination via unique mechanisms, and it is likely that in the absence of an intact immune response, some strains of MHV infection in the CNS are responsible for the onset of demyelination, possibly through the direct destruction of OLGs. MHV-induced demyelination can serve as a model for oligodendroglial tropic, nonimmune-mediated mechanisms of demyelination that may have important relevance for our understanding of MS.

5. MHV Pathobiology

MHV is a member of the coronavirus family [44–46]. The virus infects many vertebrate hosts and induces a variety of diseases ranging in severity. The outcome and degree of MHV-induced disease are dependent on several factors, including the age and strain of the mouse, the strain of MHV, and the route of virus inoculation. Even very closely related strains of MHV differ in pathogenic properties. Some strains of MHV are purely hepatotropic (e.g., MHV-2) [47]; some are primarily neurotropic (e.g., JHM, MHV-4, an isolate of JHM) [22, 48]; while others (e.g., MHV-A59 and MHV3) [21, 49] are both hepatotropic and neurotropic.

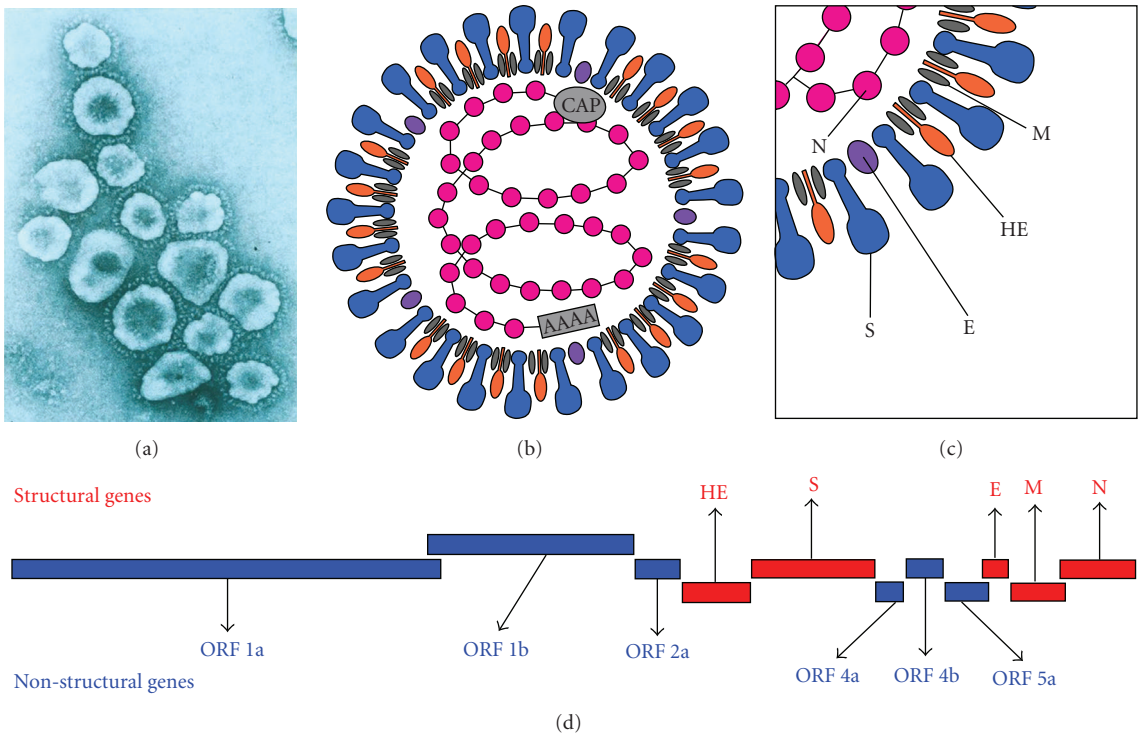

Figure 1: MHV virion and MHV genome: (a) electron micrographs of coronavirus particle. (b, c) Schematics of structural protein organization in the MHV virion; MHV virion is somewhat pleomorphic, containing an internal helical RNA genome-nucleocapsid phosphoprotein (N) complex, surrounded by an envelope containing glycoprotein peplomer (S, E, HE, and M) as specified in the text. (d) Organization of the genes in the MHV genome; structural genes are shown in red letters and nonstructural genes in blue letters.

6. MHV Virions

MHV virions are 60–200 nm in diameter, somewhat pleomorphic (Figure 1(a)), containing an internal helical RNA genome-nucleocapsid phosphoprotein (N) complex, surrounded by an envelope containing Spike glycoprotein (S), transmembrane glycoprotein (M), envelope protein (E), and hemagglutinin-esterase protein (HE) (Figures 1(b) and 1(c)) [50]. Structural proteins expressed at the 3′ half of the MHV genome are believed to be responsible for MHV pathogenesis. S is a highly glycosylated protein. The outward radial projection of S gives the virus its family name *corona* (like a crown). HE forms smaller spike on virions, but its function in the virus life cycle is yet not clearly defined. Both M and E play a role in the assembly of virions [51]. The virions also have the I protein of unknown function [52].

7. MHV Genome

The MHV genome is a singlestranded, and non-segmented, polyadenylated RNA, of positive polarity [53]. It is one of the largest known viral RNA genomes with a length of 31-32 Kb [46, 54, 55]. The RNA genome contains 7 genes, termed 1 to 7, encoding structural as well as nonstructural genes (Figure 1(d)). There is a leader RNA sequence at the 5′ end of the genome that regulates the transcription of MHV-RNAs. The next two-thirds of the 5′ end of the genome are covered by Gene 1, which encodes a set of polyproteins with polymerase and replicase functions. Gene 2 encodes two proteins including a 30 kD product of ORF2a. Gene 2 also transcribes a 65 kD hemagglutinin-esterase protein in some MHV strains. Genes 3, 6, and 7 code for the spike protein (S), transmembrane glycoprotein (M), and nucleocapsid protein (N), respectively. Gene 4 encodes a 12–14 kD product while gene 5 encodes a 13 kD product of a still unidentified nonstructural protein and a membrane-associated E protein. It also contains a large open reading frame embedded entirely in the 5′ half of its N gene. This internal gene (I) encodes a mostly hydrophobic 23 kD structural protein [52].

8. MHV Entry and Replication

During lytic infection, MHV enters the host cell via attachment of the S protein to specific receptors on the host pericellular surface. Carcinoembryonic antigen is one receptor implicated in infection of cultured mouse cells [56]. The receptor interaction triggers fusion of the viral and plasma membranes, allowing entry of the nucleocapsid into the cytoplasm, where all virus-specific RNA and proteins are synthesized. The nascent MHV virions acquire their membrane envelope by implanting themselves into the lumen of the intermediate compartment between the endoplasmic reticulum and Golgi complex of the host. Mature virions are thought to move through the vesicles via the secretory pathways and exit the cell when the vesicles fuse with the plasma membrane [57].

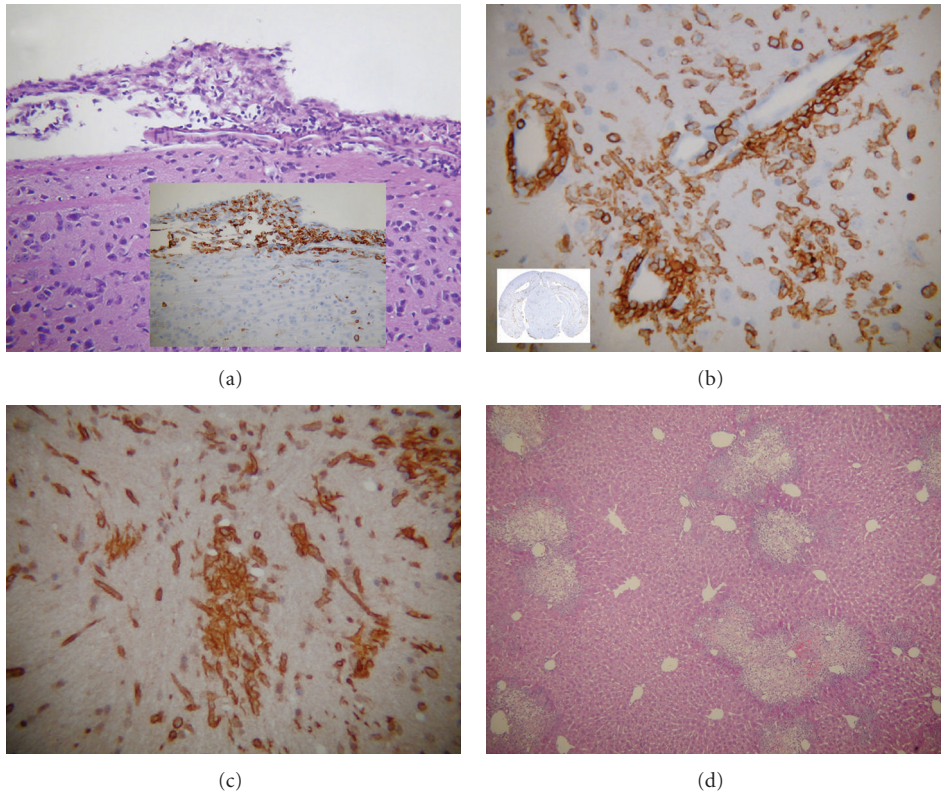

Figure 2: Archetypical histopathology of brain and liver during acute infection with neurotropic strain. MHV-A59: serial coronal sections from MHV-A59-infected mice at day 5 post infection were stained with H & E or immunostained for CD45 (LCA: leukocyte common antigen, marker for inflammatory cells) or microglia/macrophage marker CD11b (OX42). (a) H & E staining shows acute meningitis and inset shows the presence of inflammatory cells positive for LCA. (b) Coronal sections stained for LCA show acute encephalitis in brain section characterized by the formation of perivascular cuffing in high magnification. Inset shows presence of inflammatory infiltrates throughout the parenchyma. (c) The majority of LCA-positive inflammatory cells are stained positive for the macrophage/microglia marker CD11b in MHV-A59-infected brain parenchyma. (d) Liver pathology from the same infected mouse stained with H & E shows lesions throughout the liver section.

9. MHV Recombination

Viral recombination has been extremely useful for systematically exploring the possible biological consequences of viral genomic differences. The recombination technique has been extensively exploited to study reovirus disease in mice, where the segmented nature of the viral RNA has enabled resorting of viruses with RNA segments from different strains with different biological properties [58]. In sindbis virus and picornaviruses, a full-length infectious clone of the viral genome has been exceptionally useful in the study of viral properties [59, 60].

In MHV, the replicase carries out "discontinuous transcription" in the fusion of body and leader sequences in subgenomic RNAs and also during recombination events which occur at high frequency during MHV replication. High-frequency RNA-RNA genomic recombination events are archetypal for coronaviruses [61]. These serve as mechanisms of virus evolution and modulation of viral pathogenesis, a largely unexplored area of study which offers deep insight into the genomic control of biological properties. But for a long time the large genome size was a technical obstacle to achieving such a goal with coronaviruses. This problem was circumvented by molecularly cloning defective interfering-like RNA, leveraging the high RNA recombination frequencies during mixed infection. This targeted recombination technique in MHV was developed by Dr. Paul S. Masters and colleagues and used extensively to introduce alterations into the 3′ end of the MHV genome [62–64]. It was able not only to exchange specifically the structural and non structural genes among the MHV strains but also to introduce single amino acid substitutions. In the last few years there have been reports of full-length infectious clones for many coronaviruses including MHV and a human coronavirus causing severe acute respiratory syndrome (SARS) [65–69].

10. MHV Pathogenesis

10.1. Meningoencephalitis, Demyelination, and Axonal Loss. Upon intracranial (i.c) infection of neurotropic MHVs acute meningoencephalitis (with or without hepatitis) is the major pathologic process (Figure 2). Viral titer reaches its peak at days 3 and 5 post infection (p.i) [47]. Infectious virus is cleared within the first 10–14 days; however, at this time mice begin to develop demyelination, either clinical or

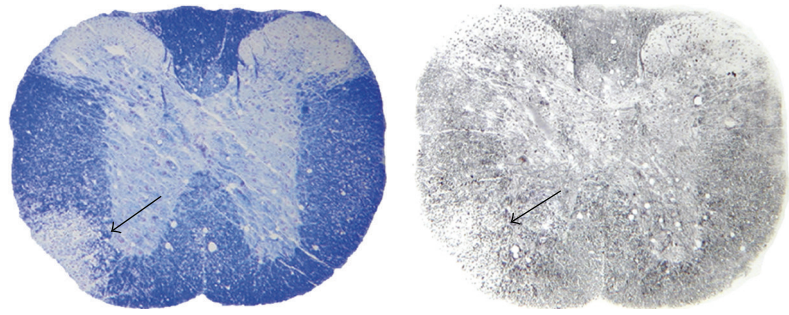

(a) (b)

Figure 3: Demyelination and axonal loss in a neurotropic strain of MHV, *MHV-A59-infected mouse spinal cord.* Serial cross-sections (5 μm thick) from MHV-A59-infected mouse spinal cord at day 7 p.i. were stained for myelin with LFB or by Bielchowsky silver impregnation. (a) A large demyelinating plaque observed in MHV-A59-infected mouse spinal cord is shown (arrow indicates demyelinated area). (b) In an adjacent section, the same demyelinating plaque of MHV-A59-infected spinal cord shows loss of axons (arrow indicates area of axonal loss) (adapted from the work of [73]).

accompanied by chronic hind limb paralysis [21, 70]. Both MHV-JHM and MHV-A59 cause inflammatory demyelination in the brain and spinal cord (Figure 3(a)) whereas MHV3 only causes vasculitis [49, 71].

It was formerly believed that in primary MHV-induced demyelination neuronal axons remain relatively preserved. Recently, it has been observed that adoptive transfer of spleen cells from immune MHV B6 mice into MHV-infected RAG − / − mice (that are defective in recombinase activating gene 1 expression, and thus lack mature B or T cells) resulted in demyelination with increased axonal damage [72]. They also showed that axonal damage is, in large part, immune mediated in MHV-infected mice and occurs concomitantly with demyelination. Concurrent axonal loss and demyelination have recently also been observed with S protein recombinant DM strain-infected mouse spinal cord as shown in Figure 3 ((a) demyelination; (b) axonal Loss) [73].

10.2. Role of Immune Cells in Viral Clearance and Demyelination. MHV clearance requires both CD8+ and CD4+ T cells [74–76]. CD4+ T cells are necessary for proper CD8+ T cell activation, survival, and retention in the infected CNS [75]. Clearance of infectious virus is mediated by both cytolytic- and cytokine-mediated mechanisms. Exact mechanisms of MHV-induced demyelination are unclear although both macrophages and T cells modulate pathologic changes [41, 77]. Severe combined immunodeficient (SCID) mice, Rag-1 knockout mice, and UV-irradiated mice infected with MHV-JHM have few lesions 7–15 days p.i despite viral replication [40, 41, 76–78]. These data suggest that lymphocytes are required for demyelination. However, demyelination mediated by $\gamma\delta$T cells still occurs in nude mice that lack CD4+ and CD8+ T cells [79]. Interestingly, demyelination occurs to a similar extent in wild type, B cell-deficient, and Rag-1 knockout mice and in mice lacking antibody receptors or active complement pathways, when infected with MHV-A59 [42].

10.3. Viral RNA Persistence During Chronic Demyelination. Viral RNA persistence is essentially the failure of the immune system to clear viral RNA from infected organs, mainly the CNS. Viral RNA persistence has been demonstrated in infections with all of the neurotropic demyelinating strains of MHV including JHM and MHV-A59 [24, 25, 80]. Viral RNA persistence appears to be an important factor and perhaps even a prerequisite for MHV-induced demyelination during chronic immune-mediated demyelination. MHV strains that do not persist, such as MHV-2 and Penn 97-1 (laboratory recombinant strains of MHV) [81, 82], also do not demyelinate. However, the persistence-positive, demyelination-negative phenotypes of Penn 98-1 and Penn 98-2 (S protein recombinant strain of MHV) [81] indicate that viral persistence per se is insufficient to induce demyelination. Penn 98-1 and Penn 98-2 (S protein recombinant strain) [81] may persist in neuronal cells of gray matter while demyelinating strains, such as MHV A59, persist in white matter, suggesting that cell-specific persistence is necessary for demyelination. During chronic infection, MHV RNA persistence in the white matter has previously been demonstrated [25]. However, it is not known which glial cells are mainly responsible for the induction of demyelination.

10.4. Glial Cell Interaction in the Induction of Demyelination. A temperature-sensitive demyelinating mutant of JHM is known to infect mainly nonneuronal cells and specifically to have a strong affinity for astrocytes as well as to cause white matter lesions in the mouse [83, 84]. On the other hand, neurotropic nondemyelinating MHV3 has an in vitro affinity for neurons, ependymal cells and meningothelial cells but not for astrocytes or oligodendrocytes. MHV3 can induce an initial ependymitis, meningitis, and encephalitis in the absence of white matter lesions [49]. These observations reinforce the importance of glial cell infection in the onset of demyelination. Astrocytes and microglia play an important defensive role in MHV pathogenesis by secreting cytokines

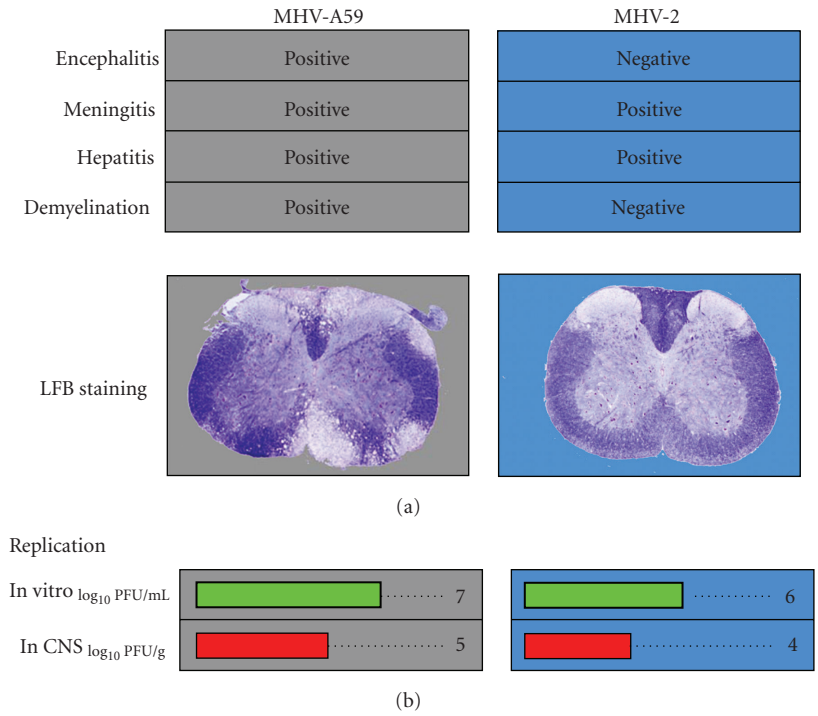

Figure 4: Index of differential pathogenesis and replication of archetypical neurotropic strain, MHV-A59 and nonneurotropic primarily hepatotropic strain, MHV-2.

[85–87]. Cytokines are believed to aid in host defense against MHV by contributing to elimination of the virus from the CNS. It has been reported that specific cytokines and chemokines (such as Interferon α, β, and γ), tumor necrosis factor (TNF-α), IL-2, Il-6, IL-1α, and IL-1β are all induced during the acute stage of MHV infection in the CNS [88]. TNF-α, IL-6, and IL-1β are reportedly secreted by astrocytes of persistently infected spinal cords [89]. The role of individual CNS cells in the induction of demyelination remains to be further elaborated.

11. Comparative Characterization of Natural and Recombinant Demyelinating (DM) and Nondemyelinating (NDM) Strains of MHV to Understand the Mechanisms of Demyelination and Axonal Loss

Natural and genetically constructed recombinant MHV strains (generated by targeted RNA recombination) with differential pathological properties were used to understand the mechanisms of demyelination and concomitant axonal loss. These encompass both demyelinating (DM) and nondemyelinating (NDM) strains of MHVs, on which we have performed comparative studies correlating the phenotypes, genomic sequences, and their pathogencity. As a first step mice were inoculated mice with plaque-purified demyelinating strain MHV-A59 [21] and nondemyelinating strain MHV-2 [90]. MHV-A59, a wild type parental strain of MHV, infects a variety of cell types, including neurons, astrocytes, oligodendrocytes, microglia, and ependymal cells [21, 70, 91, 92] in the central nervous system (CNS) and causes acute meningitis, encephalitis, hepatitis, and chronic demyelination. In contrast, MHV-2, a closely related fusion negative [93] strain to MHV-A59, has limited ability to invade brain and spinal cord, causing meningitis without encephalitis or demyelination [47, 82] but causing severe hepatitis (Figure 4), making it an appropriate experimental negative control for our understanding of mechanisms of MHV-A59-induced CNS inflammatory disease processes.

11.1. Inflammation in the Brain. Anti-CD45 (LCA: leukocyte common antigen) staining confirmed that the increased cells in the meninges of MHV-A59 (Figure 5(a)) or MHV-2-infected CNS (Figure 5(b)) consist predominantly of infiltrating inflammatory cells (Figures 5(c) and 5(d)). MHV-A59 also induced focal acute encephalitis, characterized by inflammatory infiltrates in brain parenchyma with perivascular cuffing (Figures 5(e) and 5(g)) whereas, MHV-2-infected brain inflammatory cells were restricted to the meninges, choroid plexus, and subependymal region with minimal, if any, invasion of brain parenchyma (Figures 5(f) and 5(h)). The majority of infiltrating cells were CD11b+, a macrophage/microglia marker (Figures 5(i) and 5(j)). Some CD3-stained infiltrating T cells were also found (data not shown) although nonspecific background staining of neurons with available anti-CD3 antibodies made staining difficult to quantify. Together, data suggests that MHV-induced CNS inflammation consists of mixed inflammatory cells, predominantly macrophages/microglia [73, 94].

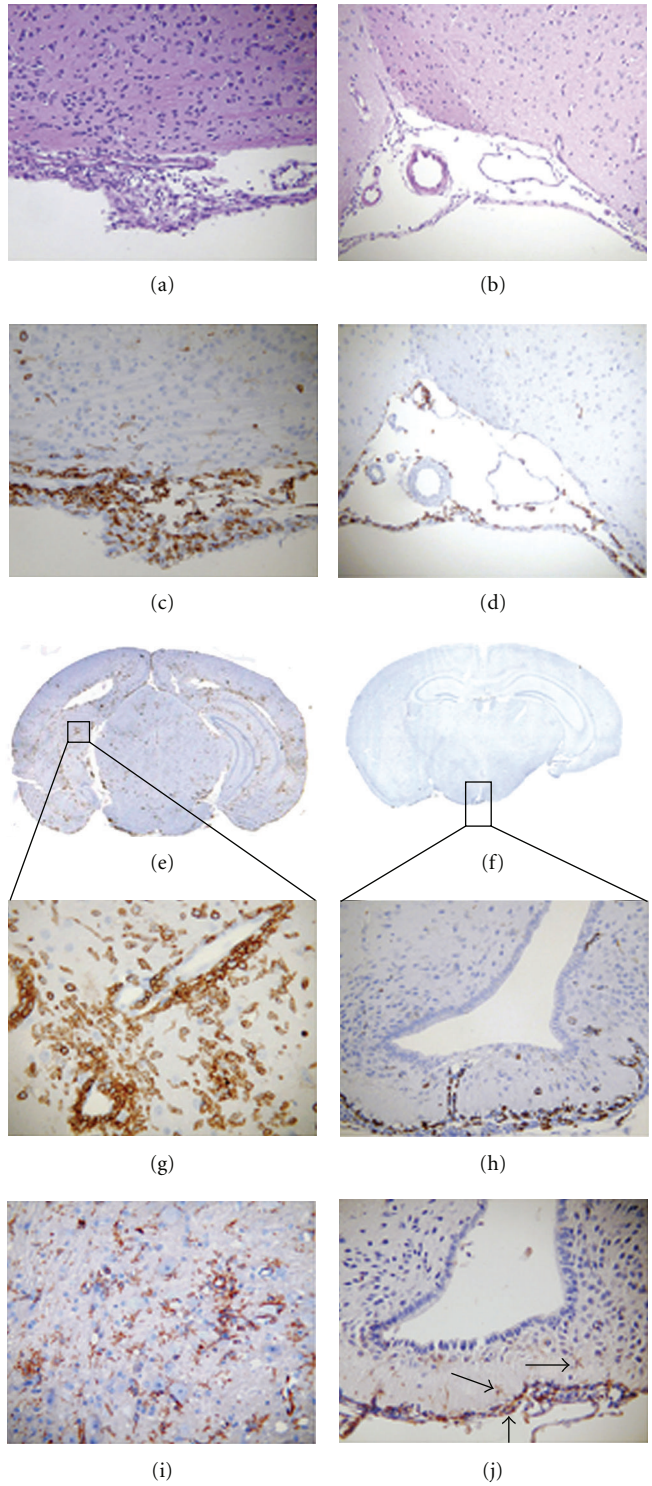

FIGURE 5: Histopathology of brain sections during acute infection with MHV-A59 compared to MHV-2. 5 μm thick serial coronal sections from MHV-A59- and MHV-2-infected mice at day 5 post inoculation were stained with H & E (a, b) or immunostained for LCA (c–h) or CD11b (i, j). Histopathology shows acute meningitis characterized by brisk leptomeningeal inflammatory infiltration in the subarachnoid space of the basal forebrain in both MHV-A59- (a, c) and MHV-2-infected (b, d) mice. Coronal sections stained for LCA show acute encephalitis in MHV-A59-infected mouse brain characterized by the presence of inflammatory infiltrates throughout the parenchyma (e) and formation of perivascular cuffing (g) in high magnification whereas in MHV-2 infection infiltrating inflammatory cells were rarely observed in brain parenchyma (f) and, when present, were restricted to the subependyma (h). The majority of LCA+ inflammatory cells stained positive for the macrophage/microglia marker CD11b in MHV-A59-infected brain parenchyma (i) and the few positive cells in MHV-2-infected brain (j) remained restricted to subependyma (arrows). Original magnifications for (a–d) and (h) are 100x, for (g, i, and j) are 200x, and for (e) and (f) are laser-scanned images. (adapted from the work of [94]).

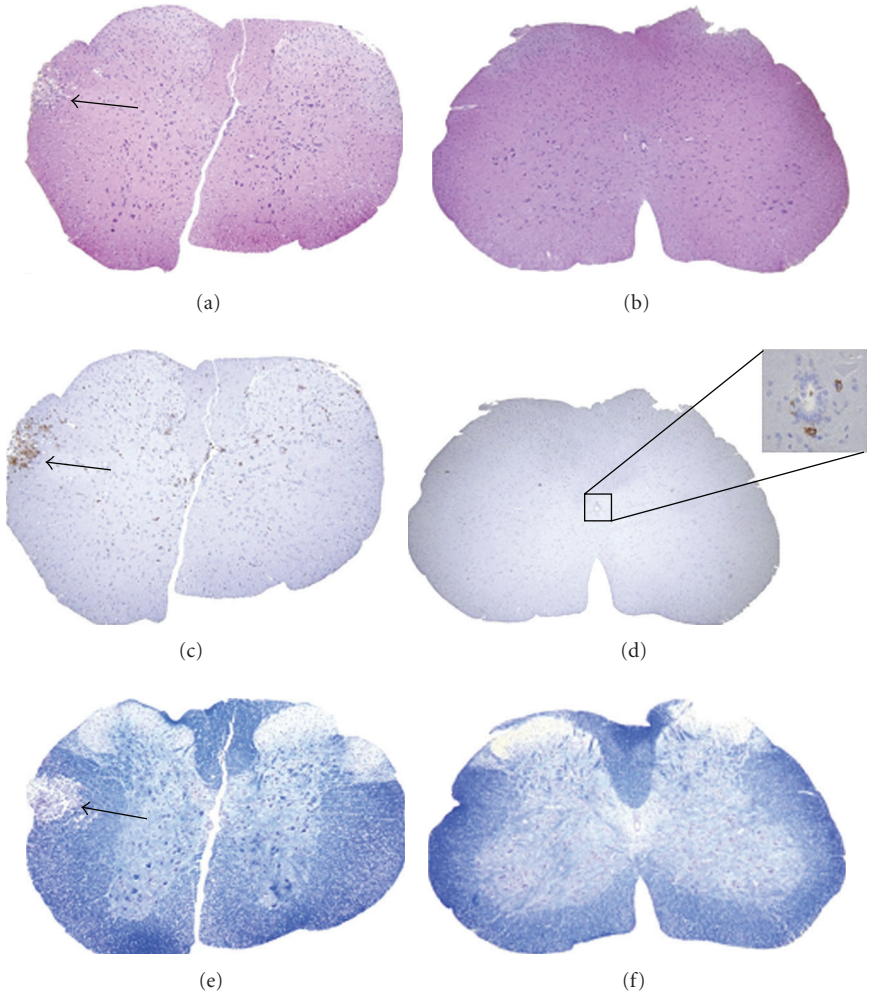

Figure 6: Comparative histopathology of MHV-A59- and MHV-2-infected mouse spinal cords. Serial cross-sections (5 μm thick) from MHV-A59- and MHV-2-infected mouse spinal cord at day 5 post inoculation were stained with H & E (a, b), LCA (c, d), or LFB (e, f). Several inflammatory lesions (a) with infiltrating LCA+ cells (c) were observed in MHV-A59-infected mouse spinal cord (arrows indicate lesion area) whereas in MHV-2-infected mouse spinal cord no parenchymal lesions were observed (b), with only rare LCA+ infiltrates observed near the central canal (d). An adjacent section of MHV-A59-infected spinal cord shows loss of myelin by LFB staining ((e) arrow indicates demyelinated area) whereas normal myelin was observed in MHV-2-infected mouse spinal cord (f). Original magnification of (a–f) is 40x. (adapted from the work of [94]).

11.2. Inflammation in the Spinal Cord. Pathology was also assessed in cross-sections of spinal cord from cervical, thoracic, and lumbar regions. Similar to brain, H & E and LCA staining demonstrated that both MHV-A59 and MHV-2 induced meningitis whereas only MHV-A59 induced myelitis (Figures 6(a) and 6(c)). In MHV-2 infection, inflammatory cells were rare and restricted near the ependymal cell lining of the central canal (Figures 6(b) and 6(d)). Similar to the brain, the majority of inflammatory cells in MHVA59 were CD11b+ (Figure 6(c)). Luxol fast blue (LFB) staining was performed to visualize myelin [94]. Demyelinating plaques developed as early as day 5 post inoculation in MHV-A59-infected mice (Figure 6(e)), with no demyelination in MHV-2-infected mice (Figure 6(f)). Day 30-post inoculation tissue sections from MHV-A59-infected mice showed a similar pattern of demyelination as on day 5, but the number and area of plaques were larger, and MHV-2-infected mice did not exhibit any demyelination. To avoid a high mortality rate of MHV-2 due to hepatitis, 0.5 LD50 doses (50 PFUs) were used. However, to ensure that the inability of MHV-2 to cause encephalitis or demyelination is not dose dependent, mice were also inoculated with MHV-A59 at 50 PFUs. MHV-A59 produced larger demyelinating lesions given at 2,000 PFUs than at 50 PFUs, but with both doses, 100% of mice were affected. Results confirm earlier findings that MHV-A59 induces demyelination whereas MHV-2 is nondemyelinating at day 30 [47]. Demyelination was not previously assessed at earlier time points. Demyelination begins as early as day 5 post inoculation, indicating that MHV-A59-induced myelin damage begins at the time of acute inflammation, similar to what is observed in MS and EAE lesions [95].

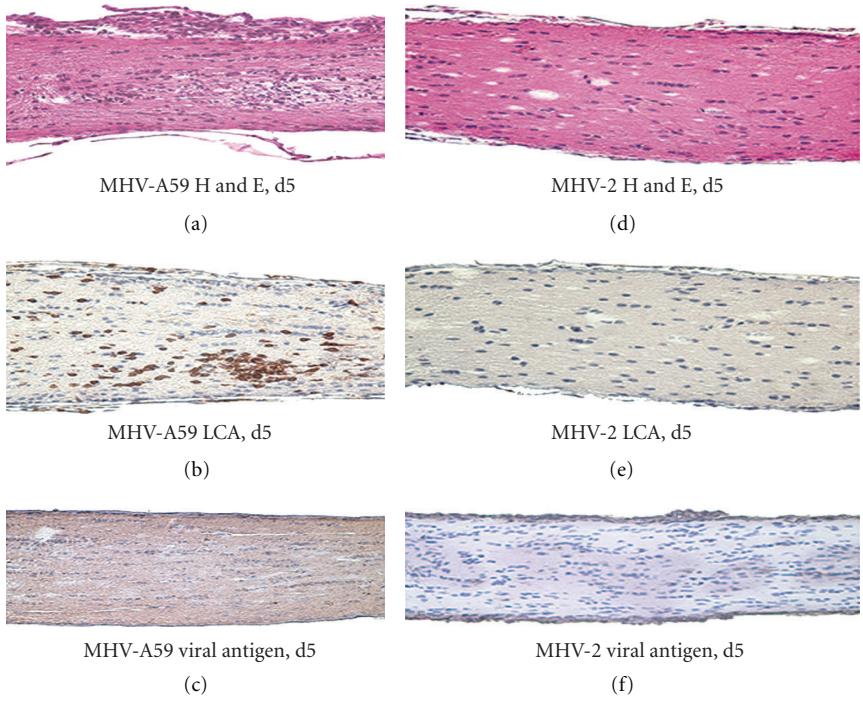

Figure 7: Optic nerve histopathology from MHV-A59-infected and MHV-2-infected mice. Longitudinal sections (5 μm thick) of optic nerve from MHV-infected mice are shown. Numerous inflammatory cells are evident in an MHV-A59-infected optic nerve with ON 5 days post inoculation stained by H & E (a) and LCA (b). Optic nerve, 5 days post inoculation, with MHV-2 (d) shows a lack of inflammation, with no LCA staining (e) detected. Viral antigen staining of optic nerve from an MHV-A59-infected mouse (c) shows low-level axonal staining whereas no viral antigen is detected in MHV-2-infected (f) mouse optic nerve. Photographs shown at original magnification x20. (adapted from the work of [94]).

11.3. Optic Nerve Inflammation. The presence of LCA+ inflammation and associated demyelination in brain and spinal cord led to hypothesize that MHV-A59-infected mice may develop optic neuritis (ON) similar to experimental ON in EAE mice. Optic nerves from MHV-A59- and MHV-2-infected mice were cut into 5 μm longitudinal sections and stained with H & E and inflammatory cell markers. For comparison, relapsing EAE was induced in 8-week-old SJL/J mice by immunization with proteolipid protein peptide as described previously in [96]. Mice were sacrificed on day 11 post immunization, when incidence of ON peaks and optic nerves were isolated. Inflammatory cells infiltrating the optic nerve sheath and parenchyma are shown by H & E and LCA staining (Figures 7(a) and 7(b)) 5 days post inoculation with MHV-A59, similar to inflammation seen in EAE ON [94]. In contrast, optic nerves from MHV-2-infected mice did not develop ON (Figures 7(d) and 7(e)), with histological appearance similar to control optic nerves. Both CD11b+ and fewer CD3+ cells were noted in MHV-A59-infected optic nerves similar to brain. By day 15 post MHV-A59 infection, optic nerve inflammation completely resolved. Detection of viral antigen in optic nerves was limited to axons because there are no neuronal cell bodies present. Light diffuse staining detected in optic nerves from MHV-A59-infected mice (Figure 7(c)), but not MHV-2-infected mice (Figure 7(f)), suggests that MHV-A59 viral antigen is likely present in optic nerve axons. Consistent with the observed pattern of inflammation, optic nerves from MHV-A59-infected mice had areas of demyelination detected by LFB staining 30 days post inoculation whereas no demyelination occurred in MHV-2-infected mice. The degree of optic nerve inflammation was scored on a 0 (no inflammation) to 4 (severe inflammation) point scale described previously in [96–98], with any amount of inflammation (score 1–4) considered positive for ON. ON was detected as early as 3 days post inoculation with MHV-A59, with peak incidence at day 5 (Figure 8(a)) and resolution by day 15. At the peak of ON (day 5), almost 50% (10 of 21) of optic nerves examined from MHV-A59-infected mice had ON (Figure 8(b)), with an average relative inflammation score of 1.7 ± 0.21 whereas, only one of 21 nerves from MHV-2-infected mice had even mild inflammation (score 1.0). Incidence of ON in EAE was 60% (6 of 10) with a 1.83 ± 0.31 average inflammation score, similar to prior studies [96, 98] and comparable to the incidence induced by MHV-A59 infection.

11.4. Axonal Loss and Demyelination in the Optic Nerve. To examine whether MHV-A59-induced ON also leads to axonal loss, optic nerves were stained by Bielschowsky silver impregnation, and the area of axonal staining was quantified as described previously [99]. 30 days post inoculation, MHV-A59-infected mice had significantly decreased axonal staining compared to control nerves or nerves from MHV-2-infected mice (Figure 8(c)).

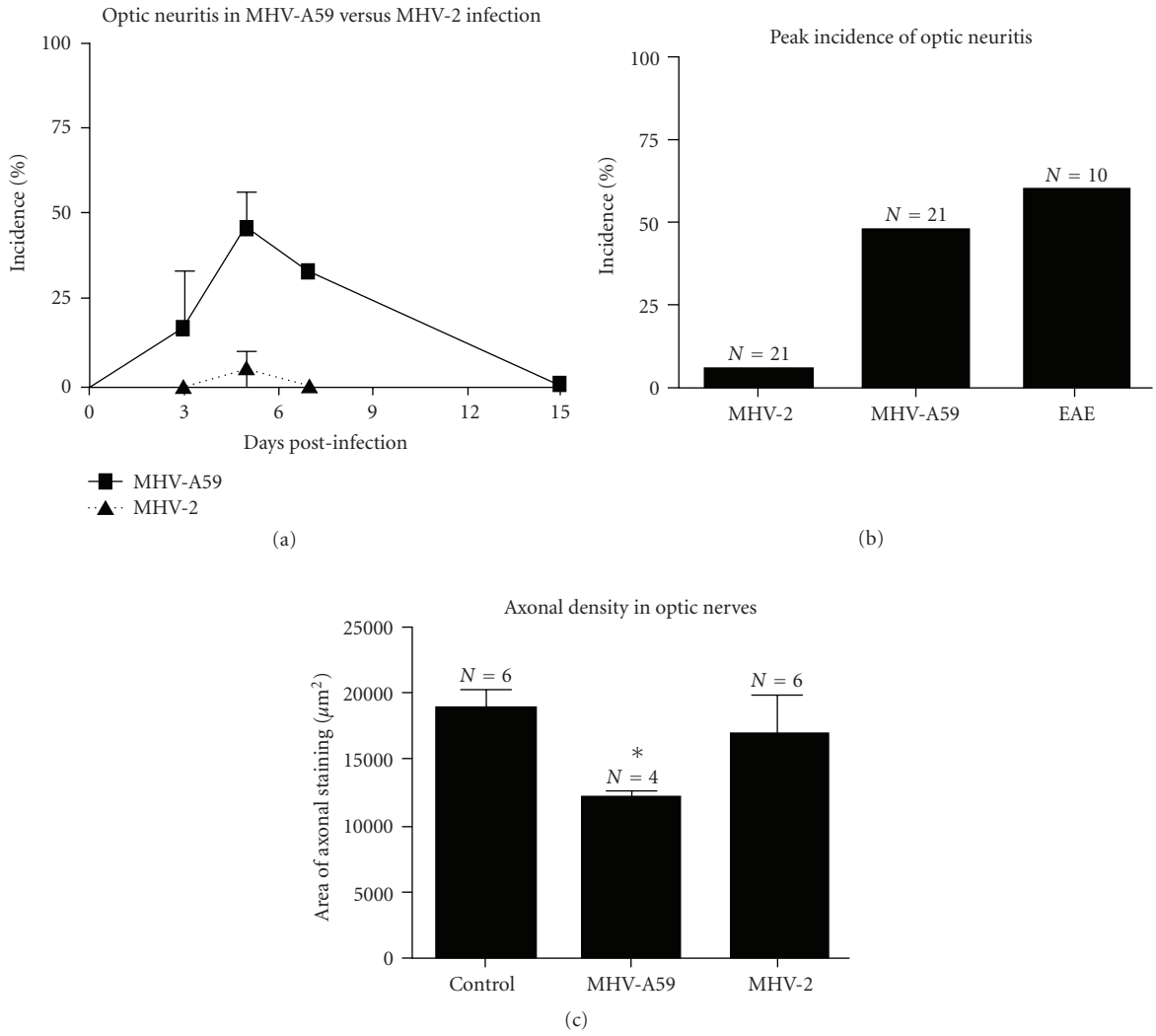

Figure 8: Occurrences of ON and axonal loss in MHV-infected and EAE mice. (a) ON, determined by presence of any level of inflammation in the optic nerve, is detected as early as day 3 post inoculation with MHV-A59. Incidence increases by day 5, persists at day 7, and resolves by day 15. In contrast, almost no MHV-2-infected mice develop ON over the same time course. Mean ± SEM incidence from 3 experiments is shown. (b) The peak incidence of MHV-A59-induced ON, detected at day 5 postinoculation, was 48% (10 of 21 nerves) whereas only one of 21 nerves from MHV-2-infected mice developed ON. 60% (6 of 10) of optic nerves from EAE (experimental autoimmune encephalitis; autoimmune model for demyelination) mice develop ON at the peak of inflammation on day 11 post immunization. (c) The area of axonal staining (mean ± SEM) detected by Bielschowsky silver impregnation is significantly lower in optic nerves from MHV-A59-infected mice as compared to optic nerves from control, uninfected mice or MHV-2-infected mice ($^*P \leq .05$). (adapted from the work of [94]).

12. Summary of Comparative Inflammatory Neuropathology of DM (MHV-A59) and Nondemyelinating (MHV-2) Strain of MHV: Insight for Understanding the Mechanisms of Demyelination and Axonal Loss

Comparative studies demonstrate that MHV-A59, but not MHV-2, induces demyelination in the CNS during acute encephalitis, as early as 5 days post inoculation, in addition to chronic demyelination previously observed at day 30 [47]. Inflammation triggered by MHV infection consists of mixed inflammatory cells, predominantly macrophages/microglia, which differs somewhat from immune-mediated models of MS where infiltrating T cells are significant contributors to pathology [95, 100]. Importantly, MHV-A59 also induces ON with similar severity and incidence as seen in the autoimmune antigen-triggered model EAE. Experimental ON is an important model being used to characterize neuronal damage and develop novel therapies for MS [98, 101–103], but studies have shown that different EAE models, induced by distinct antigens, lead to different mechanisms of RGC loss [96, 104]. The MHV-A59-induced ON model will provide a critical adjunct to study the pathophysiology of ON secondary to viral-mediated inflammation as this is one mechanism that can cause ON and MS in human patients.

13. Genomic Sequence Comparison between DM (MHV-A59) and NDM (MHV-2) Strain Provides Insight for Putative Genomic Control of Neuropathogenic Properties

Sequence comparison between MHV-2 (gene bank accession number: AF201929) and MHV-A59 (gene bank accession number 9629812) revealed 94%–98% sequence homology of the replicase genes, 83%–95% sequence homology of genes 2a, 3, 5b, 6, and 7, and a marked difference in the sequence of genes 2b, 4, and 5a among two strains. Among the structural proteins the S protein interacts with the host receptor and mediates viral-cell membrane fusion during viral entry [105]. The ~1300 amino acid spike protein in MHV-A59 is usually posttranslationally cleaved into two domains which associate with each other to form a functional dimer. In the S protein from MHV-2 strain, however, this cleavage does not occur, the reasons for which are not clearly evident. A look at the pairwise alignment between the S proteins from MHV-A59 and MHV-2 reveals that around 84% residues are common in both the chains and an additional 10% residue is similar. The 6% residues with no identity or similarity, include a 43-residue insertion in MHV-2. This insertion is by far the most significant difference in the sequence.

The role of S protein as agent of organ tropism and pathogenesis was hypothesized from comparative studies of different naturally occurring MHV strains [91, 106]. Nucleotide sequencing revealed that alterations in virus virulence were most closely associated with differences in the S gene. These findings were reinforced using targeted RNA recombination to exchange specific gene/genes of interest between different strains of MHV [107–112]. Several targeted RNA recombination studies have directly demonstrated that the S gene is a major determinant of virulence of MHV in mouse brain and liver.

14. Construction of Isogenic Recombinant Strains of MHV Expressing DM and NDM Strain S Protein

To determine whether the S gene of MHV also contains determinants of demyelination and whether demyelination is linked to encephalitis and chronic stage viral persistence, targeted RNA recombination was used to create new MHV strains, Penn 98-1 and Penn 98-2, by replacing the S gene of the encephalitic and DS (MHV-A59) with the S gene of a closely related, nonencephalitic NDS (MHV-2) [81]. Molecularly cloned vector pMH54 [111, 113], which contains the entire 3' end of the genome from MHV-A59, was used for construction of the recombinant viruses. Comparative pathological studies between recombinant DS (wtR13) and the NDS Penn 98-1 and Penn 98-2 demonstrated that Penn 98-1 and Penn 98-2 exhibit similar inflammatory infiltration (encephalitis) (Figures 9(a) and 9(b)) in the CNS during the acute stage. While wtR13 can induce demyelination at day 30 p.i. (Figure 9(c)), Penn 98-1 and Penn 98-2 are unable to induce demyelination (Figure 9(d)). Penn 98-1 and Penn 98-2 also exhibited chronic stage persistence in the spinal cord [81]. For convenience and clarity, in subsequent sections these recombinant strains were labeled in different names though they are the same but presented in different names, Penn 98-1 and Penn 98-2 are referred to as RSMHV2 (viruses expressing the MHV-2 spike in the MHV-A59 background) and wtR13 as RSA59 (viruses expressing the MHV-A59 spike in the MHV-A59 background).

As alteration of the MHV S protein influences pathogenesis, it is important to understand how alteration of the S protein alters the virus-host interaction. Previously this type of study was carried out using specific antibodies that detect viral antigen in tissues. Targeted recombination was used to select MHV isolates with stable and efficient expression of the gene encoding EGFP to facilitate the in vivo detection of virus in the mouse CNS as well as to trace the viral entry and spread in tissue culture [114]. The EGFP gene was inserted into the MHV genome in place of the nonessential gene 4, as interruption of the ORF 4 did not decrease neurovirulence in JHM [115]. The viruses replicated with similar kinetics as wild-type virus both in tissue culture and in the mouse CNS. They caused similar encephalitis and demyelination in animals as the wild-type virus or their recombinant strains; however, they were somewhat attenuated in virulence. Isogenic EGFP-expressing viruses differ only in the S gene and express either the S gene of the highly neurovirulent. Previously used names for $RSJHM_{EGFP}$ and $RSA59_{EGFP}$ are S_4R_{EGFP} and $S_{A59}R_{EGFP}$, respectively. JHM spike-mediated neurovirulence was associated with extensive viral spread in the brain [114]. The difference in virulence and patterns of spread of viral antigen between the two isogenic recombinant strains reflected the differences between parental viruses expressing each of these S genes [81, 107]. These EGFP-expressing viruses are powerful tools that can be used to follow viral spread over time without terminating infection by the fixation necessary for immunofluorescence. In order to further compare the differential pathogenesis and the CNS cell tropism between DM and NDM strain of MHV, an EGFP-expressing NDS of MHV $RSMHV2_{EGFP}$, which contains the MHV-2 (NDS) S gene in the MHV-A59 background, was constructed [114]. A cartoon representation of construction of EGFP-tagged strains of MHV has been shown in Figure 10. Detailed molecular studies show the EGFP gene is inserted and expressed at high levels that can be readily detected by microscopy [114].

15. EGFP Expressing DM and NDM Strain of MHV: A Tool to Study the Mechanisms of MHV-Induced Neuroinflammation

Frozen sagittal brain sections were obtained from $RSA59_{EGFP}$- and $RSMHV2_{EGFP}$-infected mice, postfixed, and observed by fluorescent microscopy. One of such representative EGFP expressing sagittal brain sections has been shown in Figure 11. EGFP fluorescence was observed in similar regions of the brain in mice infected with both the viruses; however, the number of infected cells differed between strains. Despite the similarity in regional

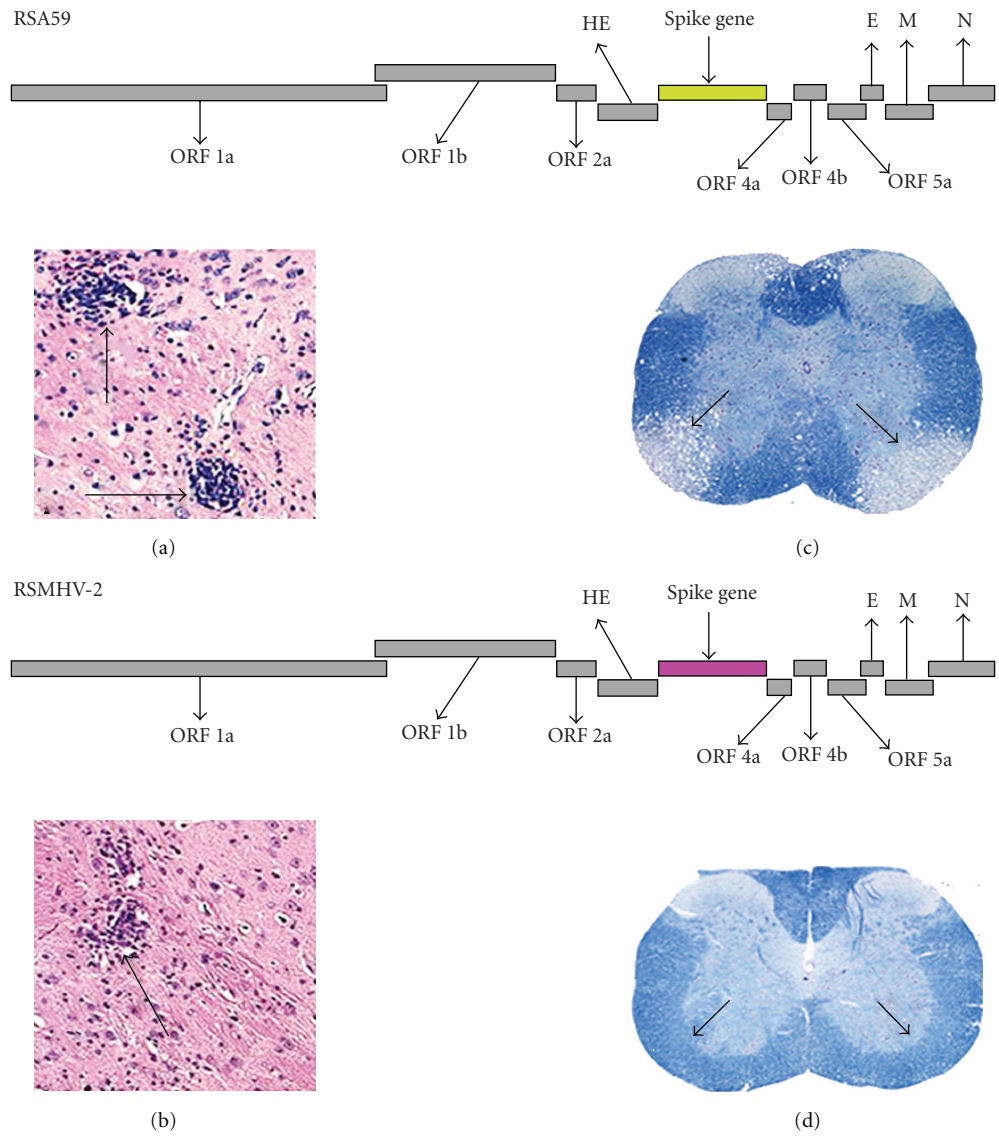

Figure 9: Comparative CNS pathology of mice infected with isogenic recombinant strains differs in the S gene. Schematic diagram of isogenic recombinant strains RSA59 (S gene denoted in green color) and RSMHV2 (S gene demoted in pink color). Encephalitis (a, b). Haematoxylin- and eosin stained brain sections from the basal fore brain of mice infected with either RSA59 (a) or RSMHV2 (b) at day 5 post infection. Arrows indicate regions of inflammation. Demyelination (c, d): spinal cord sections of mice infected with RSA59 (c) or RSMHV2 (d) at day 30 post infection were stained with Luxol fast blue. The arrows indicate a region of demyelination in (c) and normal myelinated areas of white matter in (d).

localization, the distribution of $RSMHV2_{EGFP}$ (NDM) strain is more localized in the brain parenchyma compared to $RSA59_{EGFP}$ (DM) strain.

15.1. Colocalization of EGFP Positive Cells with Viral Antigen. To confirm that EGFP positive cells were also positive for viral antigen, frozen sections were labeled with antinucleocapsid antiserum as primary antibody and Texas red goat antimouse IgG as secondary antibody. EGFP fluorescent was colocalized with viral antigen in both $RSA59_{EGFP}$-$RSMHV2_{EGFP}$ and-infected brain cortical sections (data not shown). There is a high degree of colocalization of EGFP and viral antigen in the majority of sections analyzed. Complete colocalization demonstrated that EGFP fluorescence can be used to detect viral antigen without performing any immunostaining.

15.2. Comparative Neuropathology of EGFP Expressing DM and MDM Strains. Pathology was also assessed in five to seven cross-sections of spinal cord from cervical, thoracic, and lumbar regions at day 7 (peak inflammation) and day 30 (peak demyelination) p.i. Demyelinating plaques were detected by LFB stains for myelin at day 7 p.i. in DM-infected mice (Figure 12(a)) and were quantified on a 0–3 scale [94] in four quadrants from two spinal cord levels for each mouse [116]. Day 30 p.i.-tissue sections from DM-infected mice

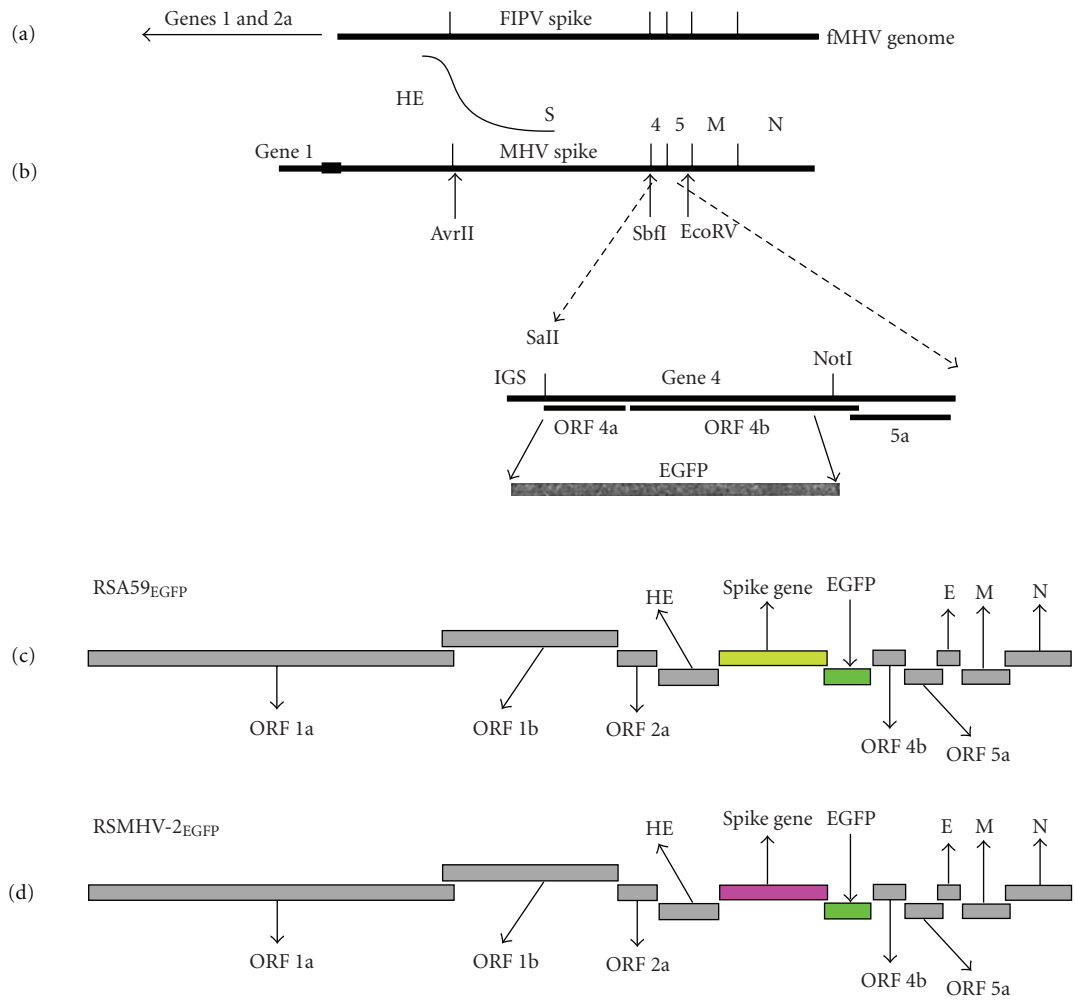

Figure 10: Schematic representation of targeted recombination to construct EGFP-expressing MHVs. The replacement of ORFs 4a and 4b with the EGFP gene was carried out by using recombinant technology, as described previously in [114]. (a) a schematic of the fMHV genome; it encodes the ectodomain of the feline infectious peritonitis spike in the background of the A59 genome. (b) shows the synthetic RNA transcribed from the vector $pMH54_{EGFP}$ (MHV-A59 S gene) or $pMHV\text{-}2_{EGFP}$ (MHV-2 S gene) [81, 114]. The curved line between the genome and the pMH54 RNA indicates the region in which the crossover must have occurred. The restriction sites relevant to the introduction of the EGFP gene are shown. The enlargement of the gene 4 region shows the modifications in which most of ORFs 4a and 4b are replaced by the enhanced green fluorescent protein (EGFP) gene. The IGS (intergenic sequence) is the site of initiation of transcription of mRNA 4. (c) and (d) show the resulting EGFP-expressing viruses: (c) $RSA59_{EGFP}$expressing the MHV-A59 S gene and (d) $RSMHV2_{EGFP}$ expressing the MHV-2 S gene. (adapted from the work of [114]).

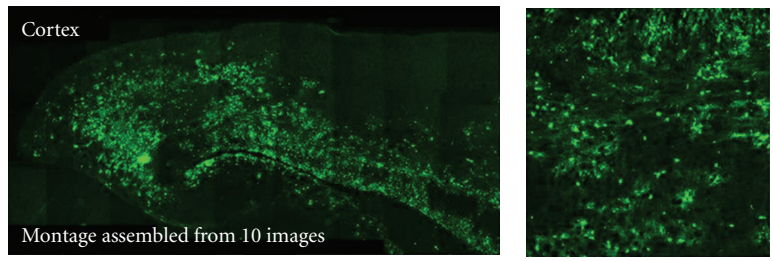

(a) (b)

Figure 11: Detection of viral antigen spread by EGFP fluorescence. Mice ware sacrificed at day 5 p.i. Brain was removed and processed for frozen sections. A portion of sagittal brain sections was cut from the middle of the brain of infected mice. Frozen sections were processed for detection of viral antigen distribution by EGFP fluorescence. Bright EGFP fluorescence was spread throughout the brain section as showed by montage assembled from 10 serial images (a). Higher magnification image (b) from the same brain section shows the cellular distribution of EGFP fluorescence. (adapted from the wprk of [114]).

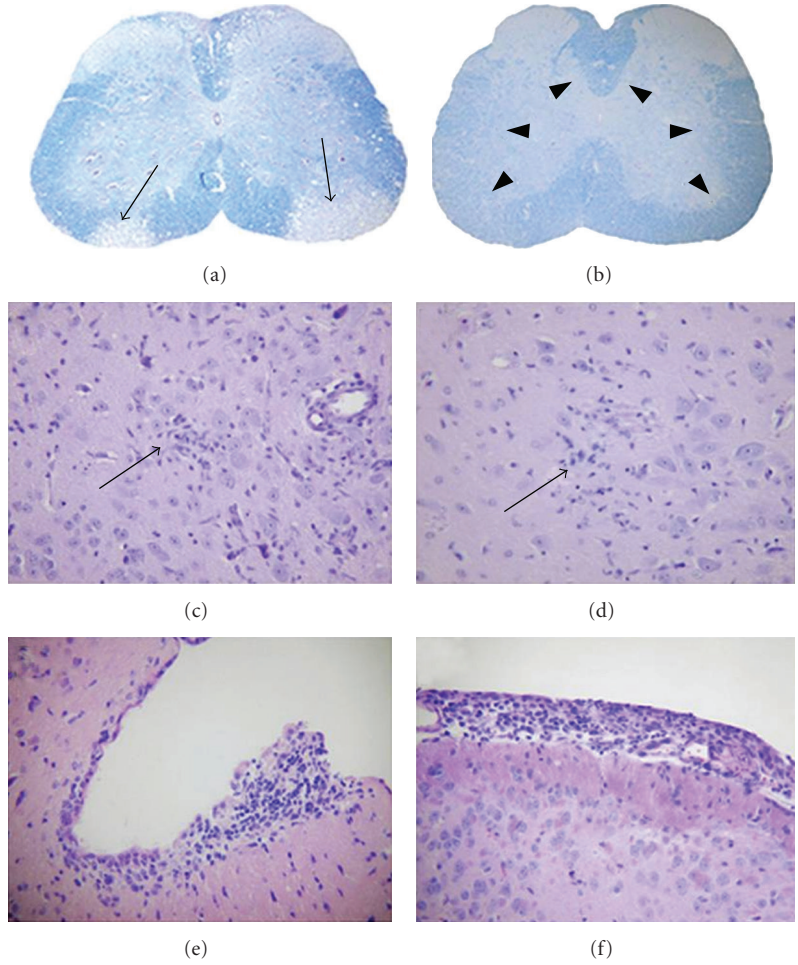

Figure 12: CNS pathology of EGFP expressing MHVs. (a, b) Demyelination: luxol fast blue-stained spinal cord sections of mice infected with $RSA59_{EGFP}$ (a) or $RSMHV2_{EGFP}$ (b), at day 30 post infection. Thin arrows indicate a region of demyelination, and the arrowheads indicate normal myelinated area of white matter. (c, d) Encephalitis: microglial nodules: Hematoxylin- and Eosin-stained sections from the basal forebrain of mice infected with EGFP tagged MHVs at day 7 post infection. Arrows indicate the microglial nodules (microglia with elongated nuclei) and lymphocytes in the vicinity of neurons in mice infected with $RSA59_{EGFP}$ (c) and $RSMHV2_{EGFP}$ (d). (e, f) Meningitis. Hematoxylin- and eosin-stained sections from the basal forebrain of mice infected with EGFP tagged MHVs at day 7 post infection: $RSA59_{EGFP}$ and $RSMHV2_{EGFP}$. In all cases, there is a brisk leptomeningeal lymphocytic inflammatory infiltrate. An original magnification for (a, b) is 20x and (c–f) is 200x. (adapted from the work of [116]).

showed a similar pattern of demyelination as on day 7, but the number and area of plaques ware larger [73]. NDM-infected mice did not exhibit any demyelination either at day 7 (Figure 12(b)) or at day 30 p.i. (data not shown) [73].

Though comparative histopathological studies demonstrated that $RSA59_{EGFP}$ could induce demyelination (Figure 12(a)) whereas $RSMHV2_{EGFP}$ cannot induce demyelination (Figure 12(b)), both $RSA59_{EGFP}$ and $RSMHV2_{EGFP}$ viruses produced meningoencephalitis (Figures 12(c)–12(f)). Brain pathology consisted of encephalitis, characterized by parenchymal lymphocytic infiltrates and microglial nodules with focal neuronophagia (Figures 12(c) and 12(d)). Brain sections from $RSA59_{EGFP}$ showed comparatively more parenchymal inflammation compared to $RSMHV2_{EGFP}$. Associated lymphocytic meningitis was also present in both the strains (Figures 12(e) and 12(f)).

15.3. Significant Axonal Loss Occurs Concurrently with Demyelination Following $RSA59_{EGFP}$ Infection. Though MHV-induced demyelination is characteristically described as sparing axons within areas of demyelination, axonal loss with demyelination in the optic nerve of MHV-A59- (parental DM) infected mice has been recently observed [94]. This led to hypothesize that DM MHV may induce axonal loss in the spinal cord. To examine this, serial sections of spinal cords from $RSA59_{EGFP}$- (DM) and $RSMHV2_{EGFP}$- (NDM)-infected mice were stained parallaly by LFB and Bielchowsky silver impregnation. DM-infected spinal cord sections at both day 7 and day 30 p.i. showed a significant decrease of axonal staining in demyelinating plaque (Figures 13(a) and 13(b)). No demyelination and no axonal loss ware evident in the NDM-infected mouse spinal cords either at day 7 (Figures 13(e) and 13(f)) or at day 30 p.i.

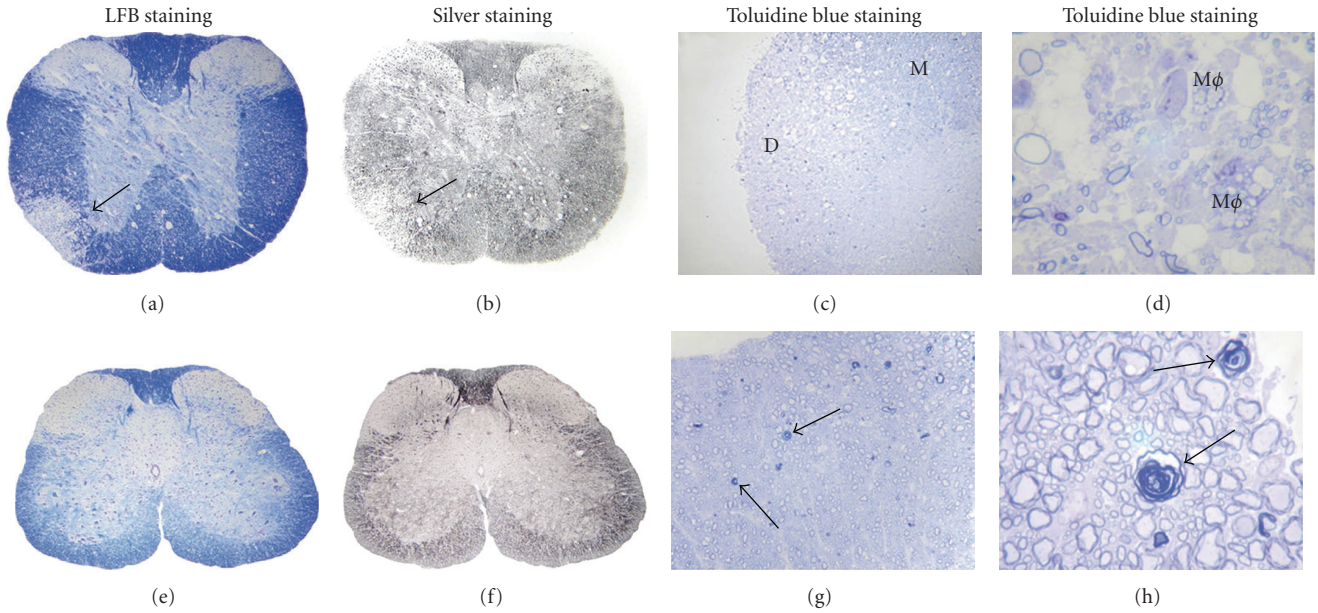

Figure 13: Demyelination and axonal loss in DM- and NDM-infected mouse spinal cord. Serial cross-sections (5 μm thick) from DM- and NDM-infected mouse spinal cord at day 7 p.i. were stained for myelin with LFB (a, e) or by Bielchowsky silver impregnation (b, f) or toluidine blue to delineate preservation of myelin, axons, and axon-myelin coherence following DM and NDM infection. (a) A large demyelinating plaque observed in DM-infected mouse spinal cord is shown (arrow indicates demyelinated area). (b) In an adjacent section, the same demyelinating plaque of DM-infected spinal cord showed loss of axons (arrow indicates area of axonal loss). (e) Normal myelin was observed in NDM-infected mouse spinal cord. (f) No axonal loss was observed in the NDM-infected mouse spinal cord. Spinal cord sections (1 μm thick) of mice sacrificed 30 days p.i. with DM and NDM were stained with toluidine blue (c, d, g, and h). Large demyelinated plaques were observed in DM-infected mouse spinal cord (C.D) . Myelinated spinal cord white matter region is marked (M), demyelinated region of spinal cord white matter (d), gray matter (g), macrophages (Mϕ). In NDM-infected mouse spinal cord, myelin remains relatively preserved with rare examples of early axonal degeneration characterized by loss of the central axon and collapse of the myelin sheath (arrows) (g, h). Original magnification for (a, b, e, and f) is 40x. Original magnification for (c, g) is 100x and fot (d, h) is 1000x. (adapted from the work of [73]).

To further evaluate the loss and/or preservation of myelin in DM- and NDM-induced inflammatory plaques, semithin spinal cord sections cut at 1-micron intervals from five infected mice at day 30 p.i. were stained with toluidine blue. Control mock-infected mouse spinal cord was used to evaluate for background fixation and/or postfixation artifacts. DM-infected spinal cords showed significant myelin loss within plaques (Figure 13(c)). Moreover, high magnification images showed infiltrating macrophages filled with myelin debris (Figure 13(d)). In contrast, in NDM strain RSMHV2-infected spinal cord sections, myelin is almost completely preserved, with only rare examples of early axonal degeneration, characterized by loss of the central axon and collapse of the myelin sheath (Figures 13(g) and 13(h)). The presence of this focal axonal degeneration was not detectable in prior studies of paraffin-embedded tissues by silver impregnation.

15.4. High-Resolution Electron Micrographic Analysis Confirms Axonal Loss Concurrent with Demyelination in RSA59$_{EGFP}$-Infected Mouse Spinal Cord. To further characterize axonal pathology at the ultrastructural level, representative foci of demyelination and axonal injury were selected from toluidine blue-stained sections, and 600 Å ultrathin sections from Poly-Bed-embedded blocks were processed for TEM. High-resolution TEM images show a combination of axonal degeneration and demyelination. There are extensive axonal loss and many residual empty vacuoles corresponding to totally degenerated fibers. In addition, there are numerous hypomyelinated fibers and naked axons without any myelin sheath, indicative of a demyelinating process (Figures 14(b)–14(d)). These naked axons are fully intact with surrounding axolemmas and axoplasm with preserved microtubules and intermediate filaments (Figure 14(e)). In contrast, NDM-infected mouse spinal cords demonstrate no appreciable axonal loss and no features of demyelination. Specifically, there are no hypomyelinated fibers, no naked axons, no macrophages, and no evidence of macrophage-mediated myelin stripping. Instead, there are only rare examples of early axonal degeneration characterized by loss of the central axon and collapse of the myelin sheath (Figure 14(f)) as previously seen in toluidine blue-stained sections. Normal myelinated region is denoted in Figure 14(a).

15.5. Macrophage-Mediated Myelin Stripping in DM-Infected Spinal Cord Section. One mechanism of demyelination is revealed as macrophage-mediated myelin stripping. This is demonstrated in Figure 15 in which a macrophage is observed surrounding a myelinated axon. The myelin is unraveling, yet the axon is completely intact. At the inner

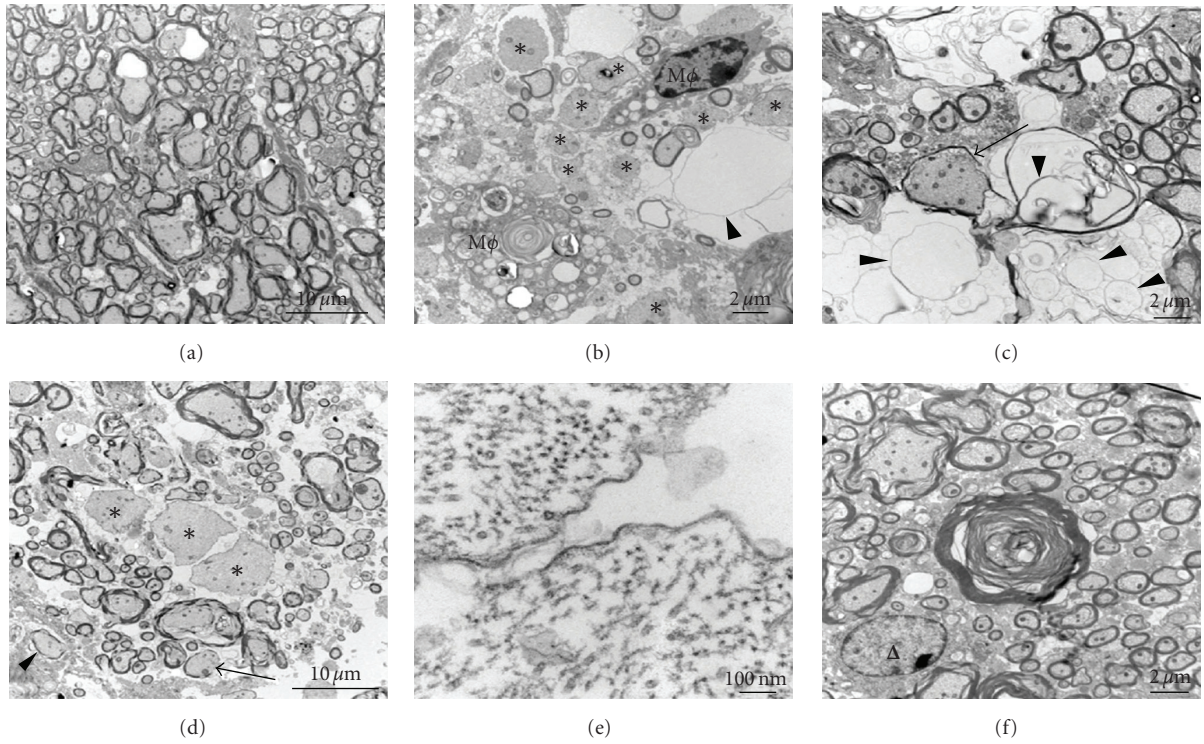

Figure 14: Electron micrographic analysis of demyelination and axonal loss in DM- and NDM-infected mouse spinal cord. Representative foci of demyelination and axonal injury were selected from the toluidine blue-stained sections shown in Figure 3 and processed for electron microscopy. (a) Normal morphology of myelinated axons was exhibited from a non plaque region adjacent to a demyelinated plaque of DM-infected mouse spinal cord. (b–d) Demyelinating plaque in DM-infected mouse spinal cord showed extensive loss of myelin, hypomyelination (arrows), complete axonal degeneration with only residual empty vacuoles (arrowheads), naked axons with no myelin sheath at all (*), and macrophages (Mϕ). (e) A high-magnification image (120,000x) of a naked axon surrounded only by a single lipid bilayer shows preservation of cytoskeleton elements (microtubules and intermediate filaments). (f) In contrast, NDM-infected mouse spinal cords show only rare examples of early axonal degeneration. $\triangle$ Marks an oligodendrocyte nucleus. Such early axonal degeneration was not observed in mock-infected mice. Original magnifications: (a) 3000x, (b) 5000x, (c) 6000x, (d) 3000x, (e) 120,000x, and (f) 6000x. (Adapted from the work of [73]).

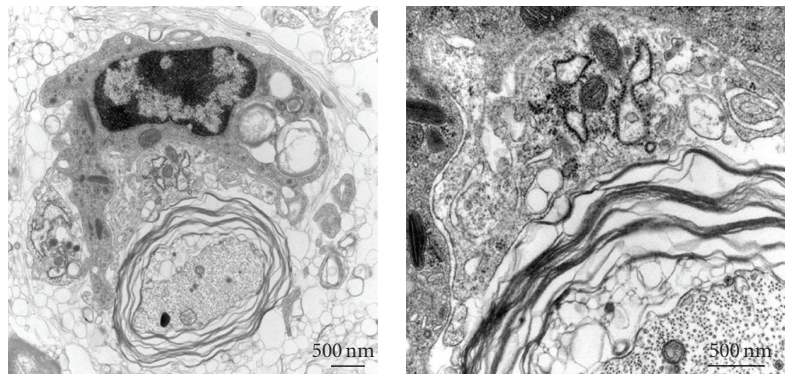

Figure 15: Macrophage-mediated myelin stripping in DM-induced demyelinating plaque. (a) A macrophage (upper portion of the figure) is observed surrounding an intact axon (lower portion of the figure) with uncompacted myelin. Myelin figures are observed within the cytoplasm of this macrophage indicative of prior engulfment of myelin. (b) Higher magnification demonstrates close apposition of the macrophage cell membrane and an outer layer of uncompacted myelin. The axoplasm and axolemma are intact and the adjacent myelin shows vesiculation indicative of myelin degeneration. Original magnification for (a) is 15,000x and for (b) is 40,000x. (adapted from the work of [73]).

border of the myelin sheath, multiple vacuoles are present as the entire myelin sheath is lifting off the axon. The macrophage cell membrane is in intimate contact with the outer portion of the myelin sheath as the macrophage strips away and engulfs the myelin sheath. Multiple vacuoles with myelin fragments are seen within the cytoplasm of the macrophage.

15.6. Spinal Cord Inflammatory Plaques Contain Predominantly Macrophages. To characterize inflammatory cells within spinal cord plaques, serial sections from DM- and NDM-infected mice were stained with anti-CD45 (LCA), anti-CD11b, or anti-CD3. LCA staining confirmed the presence of infiltrating inflammatory cells (Figures 16(c) and 16(d)). Interestingly, the distribution of LCA^+ cells was significantly different after infection by the two viral strains. At day 7 p.i., the majority of infected cells in $RSA59_{EGFP}$-infected spinal cord were localized to white matter with only occasional infiltration of gray matter (Figures 16(a) and 16(c)) whereas in $RSMHV2_{EGFP}$-infected spinal cord, LCA^+ cells were mainly restricted to gray matter (Figures 16(b) and 16(d)). CD11b staining demonstrated that the majority of LCA^+ cells in the spinal cord were $CD11b^+$ (Figures 16(e) and 16(f)). At day 30 p.i., LCA^+ cells were still present in abundance in demyelinating plaques produced following DM infection (Figures 16(g) and 16(i)), but in NDM-infected mice, no demyelinating plaques were present and very few LCA^+ cells were retained in the gray matter (Figures 16(h) and 16(j)). Immunohistochemical data demonstrate that in DM- and NDM-strain-infected spinal cord there is an increase of $LCA^+/CD11b^+$ cells; however, the distribution of these inflammatory cells is significantly different between the two strains.

15.7. DM and NDM Strains Differ in Neuronal Intracellular Distribution of Viral Antigen. To determine whether differential localization of viral antigen is responsible for the observed distribution of inflammatory cells, cross-sections from spinal cord of DM- and NDM-infected mice were examined. Since the DM and NDM viruses used in these studies express EGFP, viral distribution was assessed directly by fluorescence microscopy. On day 7 p.i., the DM fluorescence was mainly restricted to white matter (Figures 17(a) and 17(b)) with limited involvement of gray matter whereas NDM fluorescence was restricted to gray matter (Figures 17(c) and 17(d)). High-magnification fluorescence images in brain from day 7 p.i. demonstrate numerous neurons and their axons following DM infection (Figure 17(e)) whereas far fewer fluorescent neurons and axons are observed following NDM infection (Figure 17(f)). The ability of DM and NDM to replicate and spread in vitro was compared using primary hippocampal neuronal cultures and described in very recent studies . Immunostaining of MAP2b [117] and GFAP [118] demonstrated that cultures consisted primarily of neurons. At 12 hours intervals, from 0 to 72 hours p.i., cultures were monitored for viral antigen spread by fluorescence microscopy. At 24 hours p.i. several infected foci were observed in DM-infected cultures (Figure 17(g)) whereas, in NDM-infected cultures, very few discrete cells were positive for EGFP (data not shown). At 72 hours p.i., the average number of EGFP positive cells was significantly increased following infection with DM (Figure 17(h)). In contrast, NDM-infected cultures had viral infection restricted only to the initially infected neurons, with little or no spread to adjacent cells, consistent with in vivo studies (Figure 17(i)) [73].

To confirm the differential distribution of viral antigen in gray and white matter in very recent studies [116] cross-sections from several regions of all spinal cords were stained with viral antinucleocapsid antiserum. At day 5 post-infection viral antigens were mainly observed in the gray matter of the spinal cord in $RSA59_{EGFP}$- and $RSMHV2_{EGFP}$- infected mice some viral antigen was also detected in the white matter. At day 7, most of the viral antigen in $RSA59_{EGFP}$ was found in white matter whereas $RSMHV2_{EGFP}$ viral antigen remained mainly restricted to gray matter with occasional distribution to white matter. In $RSMHV2_{EGFP}$- infected mice, viral antigen was occasionally observed in the white matter, and in some spinal cord sections of $RSMHV2_{EGFP}$ viral antigen was detected at the gray-white matter junction as shown in very recent studies [116].

15.8. DM and NDM Strains Exhibit Different Cellular Tropism. The severity of tissue destruction in MHV infection is mediated by direct viral infection and immune-mediated destruction. The relative contributions of these two components differ depending on a number of virus and host factors including viral tropism, rate of viral spread, and specificity of the immune response. During acute infection, neurotropic and demyelinating strains (DM) of MHV infect a number of cell types in the CNS such as neurons, astrocytes, oligodendrocytes, and microglia [21, 70, 91, 118, 119]. Recently by using the S gene recombinant virus (S_4 R, containing S gene from a highly neurovirulent MHV-4 on the background of MHV-A59) *it has been* demonstrated that S gene-mediated neurovirulence of MHV is associated with extensive viral spread in the brain in both neurons and astrocytes [108]. Thus far it was not known whether NDM of MHV infects the same cell types as DS. The phenomenon of demyelination may be due to primary infection of a single cell type, or alternatively, infection of diverse CNS cell types leading to the final destruction of OLGs/myelin sheath and the axon.

To compare the cellular tropism of DM and NDM MHV double-label immunofluorescence on sagittal brain sections was performed [116]. EGFP fluorescence was used as a viral antigen marker, MAP2b as a neuron-specific marker, and GFAP as an astrocyte-specific marker. Sections were systematically scanned in a blinded fashion. Representative pictures of dual color fluorescence of viral antigen and MAP2b are shown in Figure 18. Visual microscopic observations show that $RSJHM_{EGFP}$ infects and spreads more in neurons in comparison to the other two strains. In $RSJHM_{EGFP}$- infected mice only a very small number of viral antigen positive cells were also positive for the astrocytic marker GFAP, whereas in $RSA59_{EGFP}$-infected mice, EGFP positive cells partially

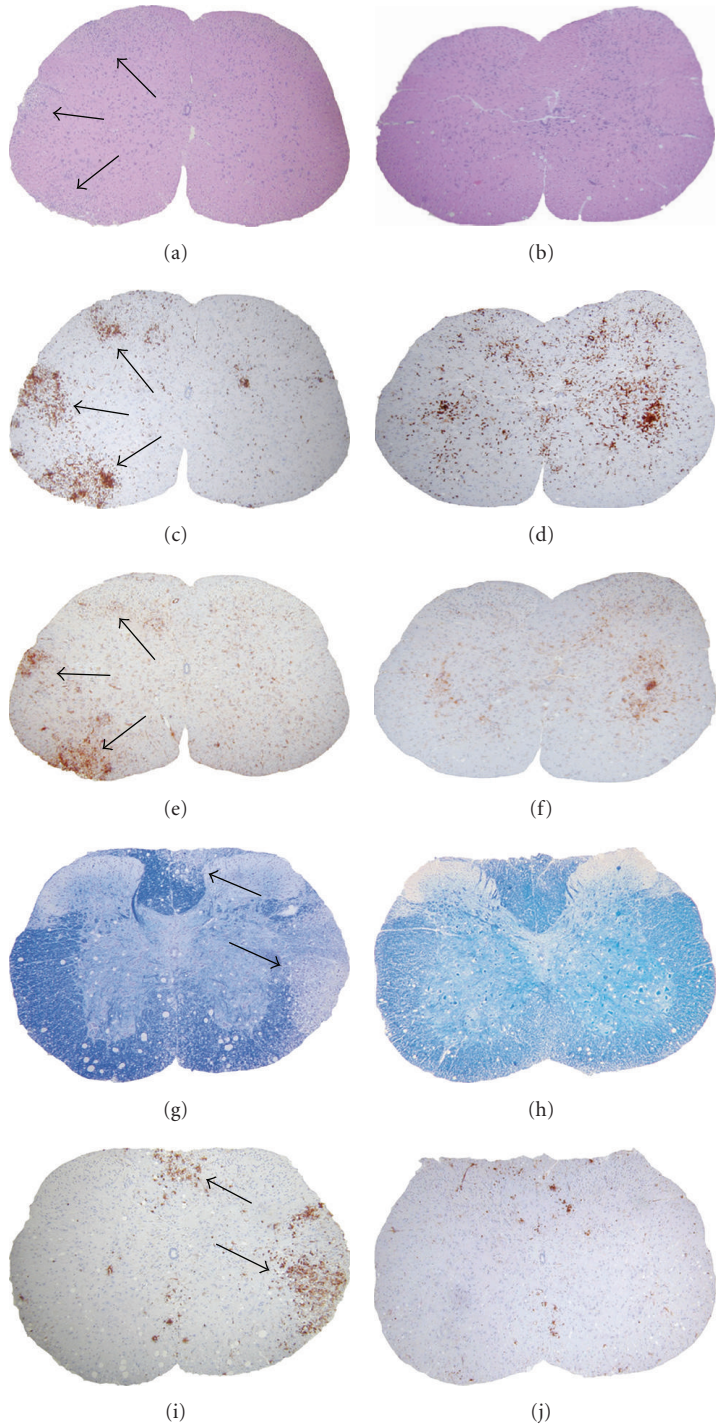

Figure 16: Distribution of inflammatory cells in the gray matter versus white matter in DM- and NDM-infected mouse spinal cord during acute infection. Serial cross sections (5 μm thick) from DM- and NDM-infected mouse spinal cords at day 7 p.i. were stained with H & E (a, b), LCA (c, d), or CD11b (e, f). Several inflammatory lesions (a) with infiltrating LCA$^+$ cells (c) were observed in RSA59$_{EGFP}$-infected mouse spinal cord (arrows indicate lesion areas in white matter). The majority of the LCA$^+$ inflammatory cells in the inflammatory plaques were positive for the microglia/macrophage marker CD11b (e). CD11b$^+$ cells in DM-infected mice are predominantly in the white matter. In NDM-infected mice no discrete inflammatory lesions were observed (b); however LCA$^+$ cells were observed (d) scattered throughout the gray matter. These cells were also strongly immunoreactive for CD11b (f). Most of the LCA/CD11b immunoreactive cells were restricted to gray matter with very little invasion of white matter. Serial cross sections (5 μm thick) from DM- or NDM-infected mouse spinal cords at day 30 p.i. were stained with LFB (g, h) or LCA (i, j). Large demyelinating lesions (g) with infiltrating LCA$^+$ cells (i) were observed in DM-infected mouse spinal cord white matter (arrows indicate lesion area) whereas normal myelin (h) was observed in NDM-infected mouse spinal cord with only rare scattered LCA$^+$ cells in the gray matter (j). Original magnification for (a–j) is 40x. (adapted from the work of [73]).

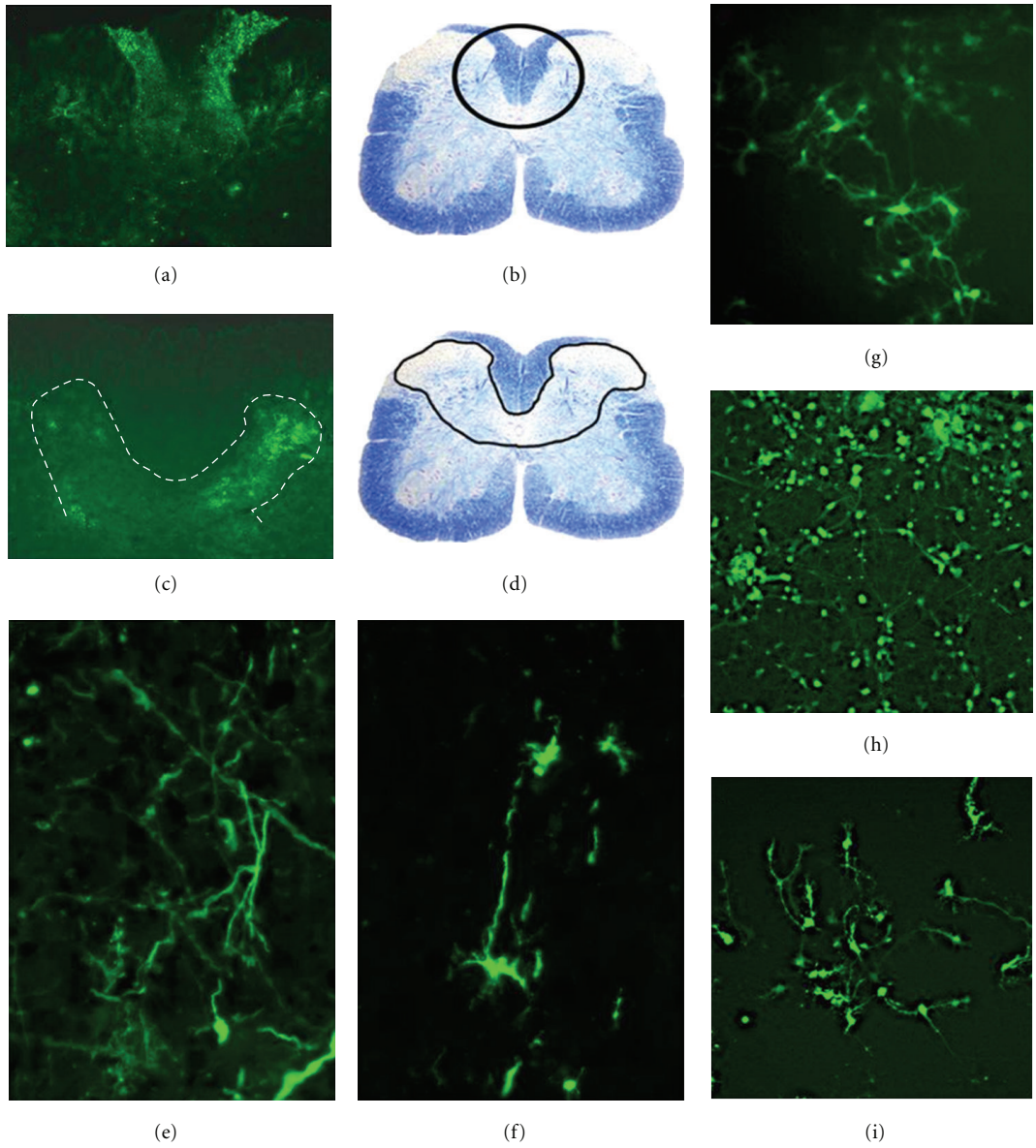

Figure 17: DM and NDM differ in their ability to translocate from gray matter to white matter during acute infection. DM- and NDM-infected mice were sacrificed at day 7 p.i.; brain and spinal cord tissues were harvested and processed for frozen sections. Cryostat sections were post fixed with 95% ice-cold ethanol for 20 minutes and observed by fluorescent microscopy for viral antigen (EGFP fluorescence). (a) In DM-infected spinal cord, viral antigen positive EGFP-expressing cells are present in both gray and white matters. (b) Area of EGFP positive cells from (a) is marked in a corresponding LFB-stained section. (c) In NDM-infected mice, EGFP positive cells with viral antigen are predominantly restricted to the gray matter. (d) Area of EGFP positive cells from (c) is marked in corresponding LFB-stained section. (e) Axonal distribution of the EGFP fluorescent viral antigen is evident in DM-infected brain. (f) NDM-infected neurons in the brain show considerably reduced axonal transport of viral antigen. (g–i) to further confirm the ability of DM and NDM to infect neurons and spread from neuron to neuron, 4-day-old primary hippocampal neuronal cultures were infected with DM and NDM at MOI of 2. Representative fields containing an equivalent density of cells are shown in each image. (g) At 24 hours p.i. DM infect a small percentage of the neurons in culture. (h) By 72 hours p.i. DM-infected neurons were observed to spread from one neuron to the next, as nearly all cells in the culture contained viral antigen despite initial infection of only a small percentage of cells. (i) NDM-infected neurons, on the other hand, demonstrate limited axonal transport efficiency at 72 hours p.i., with only a small number of cells containing a bright concentrated signal that is retained after primary infection. (adapted from the work of [73]).

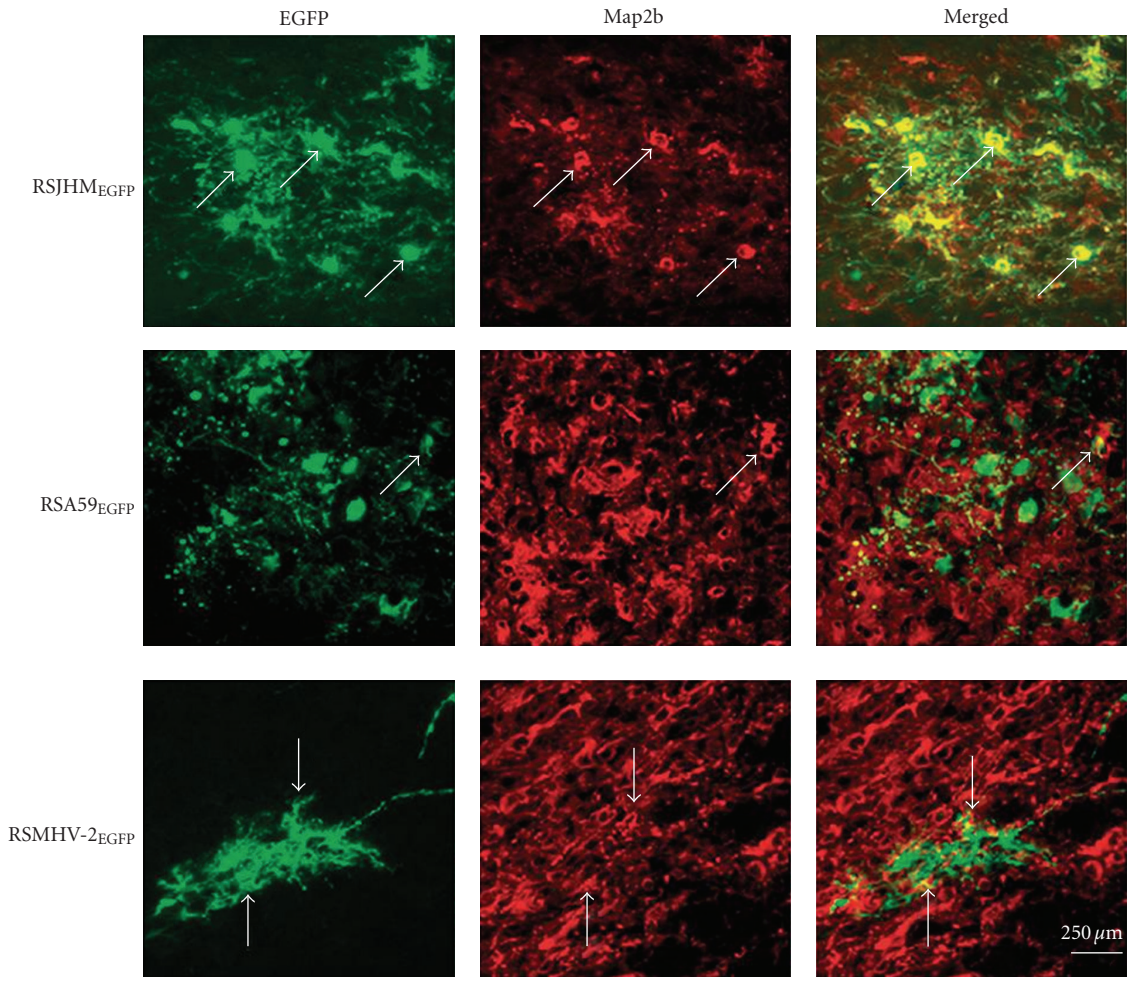

Figure 18: Identification of EGFP MHV-infected neurons in the brain at day 5 post infection. Mice were infected intracranially with RSJHM$_{EGFP}$, RSA59$_{EGFP}$, and RSMHV2$_{EGFP}$. Infected mice were sacrificed at day 5 post infection, and the brains were processed, sectioned and then labeled with anti-MAP2b as primary antiboelies and with Texas red goat anti-mouse IgG as secondary antibodies. EGFP fluorescence (green) was used to detect viral antigen-positive cells in the basal forebrain. Red fluorescence shows the corresponding labeling of MAP2b in neurons. Merged images show colocalization of MAP2b and EGFP positive cells. Arrows identify cells double positive for viral antigen and MAP2b. Bar = 250 microns. (Adapted from the work of [116]).

overlapped with GFAP staining (Figure 19). In addition, in RSA59$_{EGFP}$- infected mice EGFP positive cells were not only astrocytes but also other cell types. In contrast, in RSMHV2$_{EGFP}$-infected mice EGFP completely colocalized with GFAP (Figure 19).

Localization studies showed that MHV strains differ in their neurovirulence and ability to demyelinate and also differ in their ability to infect particular CNS cell types. RSJHM$_{EGFP}$ infects neurons with greater efficiency, and infection may spread more rapidly than in RSA59$_{EGFP}$, while RSMHV2$_{EGFP}$ infects neurons with limited efficiency. This is consistent with previous findings that the degree of neurovirulence is not only dependent on neuronal tropism but also on the number of infected neurons and spread of the infection through neurites [108]. Evidence from closely related strains of neurotropic viruses including HIV, TMEV, and reovirus supports the hypothesis that CNS cell tropism and spread in CNS cells play a major role in the distribution and type of CNS lesions [120, 121]. Studies with LCMV and HIV also suggest that virus strains that exhibit rapid spread are associated with increased immune-mediated pathology [122, 123]. Recently, it has been demonstrated that MHV spread to the spinal cord white matter occurs very rapidly, and protection from demyelination can be achieved by inhibiting this viral spread during the acute phase of infection by recruiting high numbers of MHV-specific CD8+ T cells [124]. Nondemyelinating strain is less able to infect neurons and spread through neurons; on the other hand, demyelinating strains are highly neuron tropic and spread rapidly through neurites. In contrast, it has been observed that a temperature-sensitive demyelinating mutant of JHM infects mainly nonneuronal cells, having

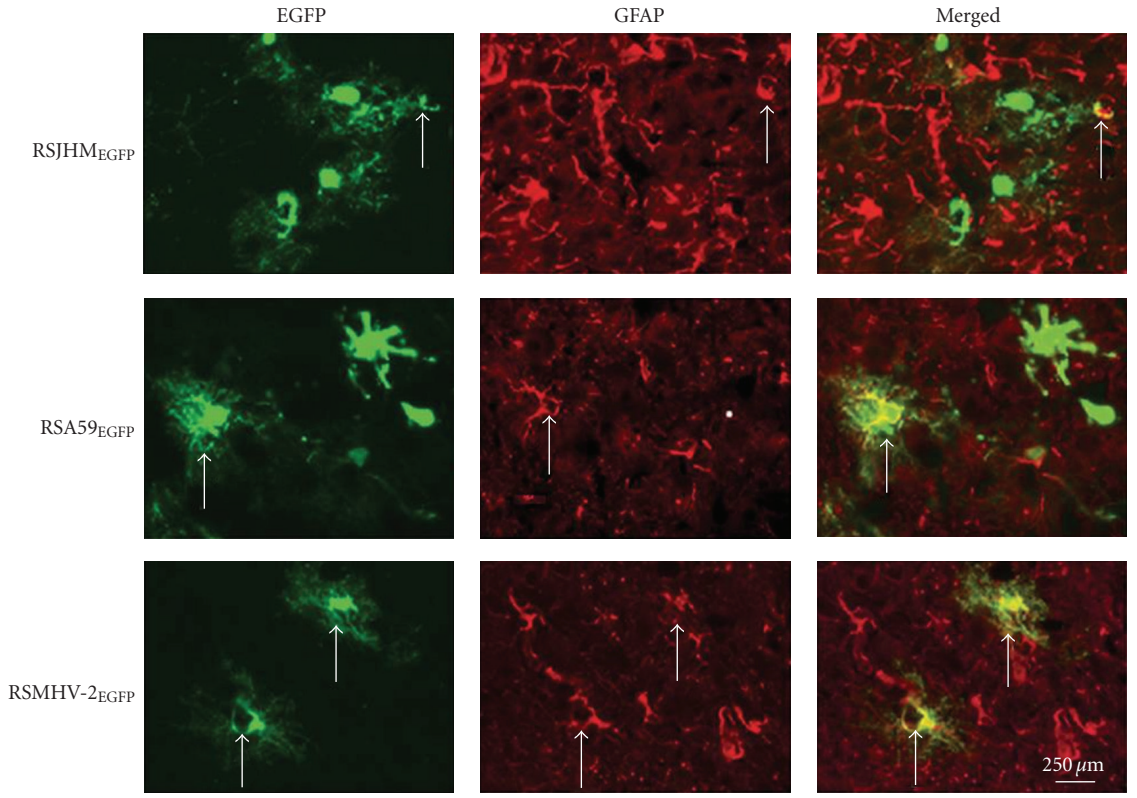

Figure 19: Colocalization of EGFP positive cells with astrocyte marker at day 5 post-infection. Mice were infected intracranially with RSJHM$_{EGFP}$, RSA59$_{EGFP}$ and RSMHV2$_{EGFP}$. Infected mice were sacrificed at day 5 post-infection; brains were processed, sectioned and then immune labeled with anti GFAP (astrocytic marker) antiserum, then stained with Texas red goat anti-mouse IgG as secondary antibodies. EGFP fluorescence was used to detect viral antigen positive cells; red fluorescence was used to detect GFAP in astrocytes. Merged images show colocalization of GFAP and EGFP positive cells. Arrows identify cells double positive for viral antigen and GFAP. Bar = 250 microns. *(Adapted from Das* [116]*).*

a strong tropism specifically for astrocytes and causes white matter lesions. Similarly, it has been demonstrated that a monoclonal antibody selected JHM variant, a S protein mutant, infects the glial cells predominantly in the CNS, causing subacute demyelination. Interestingly, the neurotropic and nondemyelinating MHV3 strain, which has an in vitro tropism for neurons, ependymal cells, and meningeal cells but not for astrocytes and oligodendrocytes, can induce initial ependymitis, meningitis, and encephalitis in the absence of white matter lesions. Our in vivo data demonstrate that the highly neurovirulent strain RSJHM$_{EGFP}$ has very little tropism for astrocytes. RSA59$_{EGFP}$ and RSMHV2$_{EGFP}$ infect astrocytes with similar efficiency. As demyelinating and nondemyelinating strains produce similar infections in astrocytes, it appears that astrocytic infection during the acute stage alone may not determine the onset of demyelination. Our observations suggest that astrocyte tropism may be a relevant factor in persistent infection but direct astrocytic infection alone may not be sufficient to induce demyelination. This study highlights the important role of neural cell tropism of viral antigen in MHV-induced demyelination in the CNS.

16. Neural Cell-Specific Viral RNA Persistence in Induction of Demyelination and Axonal Loss

The development of chronic demyelination involves replication and spread of viral antigen in the spinal cord during the acute stage of infection and the persistence of viral RNA in white matter. This is substantiated by current observations on viral spread of NDM MHV in the spinal cord, where viral antigen during the acute phase of infection is mainly restricted to gray matter. In contrast, viral antigen from demyelinating strains spreads from gray to white matter during the acute stage of infection [73, 116]. Specifically, after intracranial infection and replication, viral antigens from the demyelinating strains RSJHM$_{EGFP}$ and RSA59$_{EGFP}$ are mostly seen in spinal cord gray matter at day 5 post infection and then in the white matter at day 7 post infection. This finding establishes that demyelinating and nondemyelinating strains differ in their viral antigen distribution in gray matter and white matter during acute infection. Viral persistence observed previously in RSMHV2-infected mouse spinal cord during the chronic phase of infection may be due

to the presence of viral RNA in gray matter. Viral RNA for demyelinating strains is known to persist mainly in the white matter. Due to lack of viral RNA persistence in the white matter, essential for the induction of demyelination during chronic infection, RSMHV2 is unable to induce demyelination. It is possible that cell-specific viral RNA persistence is necessary for demyelination. These combined observations reinforce the importance of glial cell infection in the onset ofdemyelination.

17. Putative Mechanistic Aspect of DM Strain-Induced Demyelination and Axonal Loss

Based on experimental evidences it can also be argued that the spread of viral antigen from neuron to neuron and from neuron to glial cells plays a critical role in the induction of chronic stage demyelination. Both DM and NDM strains infect neurons; however, these strains differ in their capacity to translocate to white matter as determined by fluorescence of EGFP tagged viral particles. The current experiments indicate that axonal transport of viral particles is an important mechanism mediating not only the extent of axonal damage but also the subsequent induction of demyelination in the spinal cord. DM strain shows white matter involvement early (by day 7 p.i.) and at later time points that gray matter involvement is essentially absent in the spinal cord, with only minimal involvement in the brain. This observation further supports earlier findings that DM and NDM strains differ in their viral antigen distribution during acute infection in the spinal cord [116]. Evaluation of axonal loss and demyelination in the spinal cord, where there is clear separation of gray matter and large tracts of white matter, demonstrated that DM MHV infection begins in the neuronal cell body and propagates centripetally to the axon [73] which subsequently induces axonal degeneration and demyelination. NDM strains were unable to propagate from gray to white matter and as a result and were unable to induce demyelination.

The migration and activation of numerous CD11b+ macrophages/microglia to the white matter following viral spread of DM MHV [73] suggests that recruitment of these cells mediates demyelination. During DM strain chronic infection at day 30 p.i., macrophages/microglia were still present within areas of demyelination whereas macrophages/microglia and viral antigen were cleared from the gray matter following NDM strain infection.

One plausible explanation is that MHV spreads intra-axonally in an anterograde manner within gray matter and when it reaches the white matter, viral particles are able to infect oligodendrocytes via direct cell-cell contact. A less likely possibility is that infection proceeds indirectly from neurons to oligodendrocytes by intermediary cells such astrocytes, microglia, or endothelial cells. Regardless of the mechanism of viral spread, ultimately, macrophages and microglia are recruited to the areas of infection. In this way, MHV infection triggers axonal loss and macrophage-mediated demyelination. However, we have also observed in NDM strain infection, that axonal degeneration and myelin disruption can occur in the absence of macrophages. Therefore, MHV infection can both directly and indirectly cause axonal loss and demyelination. It may be that the failure of NDM strain to trigger macrophage-mediated damage is entirely a function of transport failure to the white matter.

Although there are no experimental data to demonstrate this, it can be suggested, based on our current neural cell tropism studies, that neuroinvasion by MHV may require entry into the nerve endings, transport to the cell body, replication in the cell body, axonal transport to the synapse, and transneuronal viral spread. Similar mechanisms of axonal transport of virus particles have been observed for the alpha herpesviruses, Herpes simplex virus and pseudorabies virus [125, 126]. Furthermore, Theiler's murine encephalitis virus (TMEV), a nonenveloped virus that, like MHV, causes chronic demyelination in mice, is able to traffic from the axon into the surrounding myelin in the absence of cell lysis [127]. Thus, by a mechanism involving transneuronal spread, MHV may gain access to synaptically linked neuronal circuits and glial cells. It is not clear, however, which type (s) of glial cells must be infected in order to promote the development of MHV-induced chronic demyelinating disease.

Available studies focus mainly on neurons and astrocytes, as they represent the majority of infected cells during the acute stage of MHV infection, but oligodendrocytes cannot be disregarded. It has been previously demonstrated that MHV can infect oligodendrocytes [128], but the direct cytolytic effect of MHV on oligodendrocytes is unclear [129, 130]. Direct viral infection of oligodendrocytes may contribute to MHV-induced demyelination, as observed in another human demyelinating disease, progressive multifocal leukoencephalopathy (PML), which is caused by JC virus infection of oligodendrocytes [131, 132].

18. Putative Molecular Mechanisms of Demyelination and Axonal Loss

The current studies further demonstrate that the molecular mechanisms underlying axonal damage are mediated by the S glycoprotein. The recombinant DM and NDM viruses used are isogenic on a background of the DM MHV-A59 strain and differ only by the virus-host attachment S glycoprotein. In vivo, the S protein host receptor is carcinoembryonic antigen (CEA), which functions as an intercellular adhesion molecule [56, 133, 134]. However, there is evidence that other viral entry host factors may also be permissive for viral infection [135]. Evidently, the difference in the S proteins between the DM and NDM strains does not impair host-receptor interactions or viral entry since both strains effectively cause encephalitis following transcranial inoculation. The S protein does, however, appear to play a critical role in axonal transport, with a lack of viral antigen spread and subsequent inflammation extending into spinal cord white matter following infection with the NDM strain in contrast to extensive white matter involvement secondary to DM strain infection being observed. As mentioned earlier, MHV S is synthesized as a 180kDa glycosylated precursor

that is posttranslationally cleaved into two 90kDa subunits, S1 and S2 [136], with a receptor-binding domain in the S1 subunit [137] that is responsible for the initial attachment of MHV to cell surface receptors. This binding event triggers a conformational change in S that allows S2 to initiate fusion of the virus and host membranes [138–140]. A candidate fusion peptide domain has been identified within S2 [141]; however, the actual fusion peptide for the MHV S has not been definitively identified. MHV-A59 and MHV-2 S proteins have 82% amino acid sequence identity and 94% similarity, with the S2 domain relatively more conserved and S1 more variable [93]. They also differ in their cleavage signal site whereby MHV-A59 S is cleaved posttranslationally into S1 and S2 subunits, but MHV-2 S protein is not cleaved and unable to cause fusion in vivo and in vitro. Thus, variable regions of the S1 domain or differences in the cleavage signal site between DM and NDM strains are candidate domains that may potentially explain the differential axonal transport and demyelination observed in our studies and need to be evaluated further in future studies.

Genes other than the S sometimes referred to as "background genes" also influence pathogenesis. In addition to structural proteins and replicase, all MHVs encode small unique proteins with unknown functions (ORF2a, 4, and 5a) [142]. The proteins encoded in these three ORFs appear to be nonessential for replication. It is instructive to note that, apart from the molecular role of the S gene in MHV pathogenesis, several additional genes have also been implicated in the disease etiology. Asides from their structural roles, N and M proteins are believed to function in host interactions. In porcine coronavirus, TGEV, mutations in the M protein ectodomain that impair N-glycosylation decrease the interferogenic activity and antibodies directed to the TGEV M ectodomain block IFN-γ induction [143]. For MHV, the glycosylation state of M protein may effect the ability to induce IFNγ and also to replicate in the liver [144]. In measles infection, a defective M transmembrane protein has been related to the difference in the ability of the virus to persist in the CNS and cause subacute sclerosing panencephalitis (SSPE) [145]. The N protein has been implicated in MHV-induced hepatitis [146, 147]. In addition, the replicase and other non structural proteins could affect tropism and pathogenesis by influencing the rate of viral replication perhaps by interactions with cell type specific factors or with elements of the immune response [148].

19. Conclusion

Current available studies demonstrate that the mechanisms of white matter injury in this model of CNS demyelinating disease are due to a combination of both axonal injury/loss and myelin damage. In DM infection, there is concomitant axonal loss and demyelination, and at least some demyelination is due to macrophage-mediated myelin stripping. One can hypothesize that axonal degeneration follows in this immune-mediated pathogenesis. Partial axonal loss also appears to occur secondary to direct viral-induced cytopathic effects, a non-immune-mediated mechanism. Following NDM infection, although relatively rare, myelinated fibers in the spinal cord white matter exhibit early axonal degeneration in the absence of any associated inflammation. Therefore, MHV infection exhibits diverse mechanisms of axonal loss and demyelination that are both immune and nonimmune mediated. While the underlying mechanisms leading to the development of MS in patients are not known, numerous studies have provided evidence to suggest that a viral infection may trigger this autoimmune demyelinating disease. The critical role of the S glycoprotein in viral transport and subsequent axonal and myelin damage demonstrated in the current studies suggests that targeted disruption of the S glycoprotein-host interaction has the potential to prevent the onset or progression of demyelination. Future experiments need to be geared toward identifying how the S proteins interact with the axonal transport system. Clues may be provided by other human viral neurologic infections, including those caused by such diverse viruses as Herpes Simplex and Rabies, as they take advantage of the axonal transport system in order to maximize spread and neurovirulence. Experimental mouse model provides an excellent means by which the particular host-virus interactions responsible for successful axonal transport can be dissected and clarified.

Acknowledgments

Viral-induced experimental animal model to understand the mechanism of demyelination research was supported by National Multiple Sclerosis Society, M. E. Groff Surgical Medical Research and Education Charitable Trust, and Lindback Foundation Career Enhancement Award. The success of this work has largely depended on contribution and devotion of many researchers whose names are listed in the references. Dr. Lawrence. C Kenyon is acknowledged for the pathological data analysis and Mr. Ryan Marek for image processing.

References

[1] "National Multiple Sclerosis Society-About research," June 2004, http://www.nationalmssociety.org/research-factSheet.asp.

[2] D. E. McFarlin and H. F. McFarland, "Multiple sclerosis (first of two parts)," *The New England Journal of Medicine*, vol. 307, no. 19, pp. 1183–1188, 1982.

[3] D. E. McFarlin and H. F. McFarland, "Multiple sclerosis. (second of two parts)," *The New England Journal of Medicine*, vol. 307, no. 20, pp. 1246–1251, 1982.

[4] B. Ferguson, M. K. Matyszak, M. M. Esiri, and V. H. Perry, "Axonal damage in acute multiple sclerosis lesions," *Brain*, vol. 120, no. 3, pp. 393–399, 1997.

[5] B. D. Trapp, J. Peterson, R. M. Ransohoff, R. Rudick, S. Mork, and L. Bo, "Axonal transection in the lesions of multiple sclerosis," *The New England Journal of Medicine*, vol. 338, no. 5, pp. 278–285, 1998.

[6] M. A. Hern'n, S. M. Zhang, L. Lipworth, M. J. Olek, and A. Ascherio, "Multiple sclerosis and age at infection with common viruses," *Epidemiology*, vol. 12, no. 3, pp. 301–306, 2001.

[7] B. Hemmer, J. J. Archelos, and H.-P. Hartung, "New concepts in the immunopathogenesis of multiple sclerosis," *Nature Reviews Neuroscience*, vol. 3, no. 4, pp. 291–301, 2002.

[8] D. H. Gilden, "Infectious causes of multiple sclerosis," *Lancet Neurology*, vol. 4, no. 3, pp. 195–202, 2005.

[9] J. H. Connolly, I. V. Allen, L. J. Hurwitz, and J. H. Millar, "Measles-virus antibody and antigen in subacute sclerosing panencephalitis," *Lancet*, vol. 1, no. 7489, pp. 542–544, 1967.

[10] K. G. Porter, D. G. Sinnamon, and R. R. Gillies, "Cryptococcus neoformans specific oligoclonal immunoglobulins in cerebrospinal fluid in cryptococcal meningitis," *Lancet*, vol. 1, no. 8024, p. 1262, 1977.

[11] R. T. Johnson, "The virology of demyelinating diseases," *Annals of Neurology*, vol. 36, pp. S54–S60, 1994.

[12] W. A. Sibley, C. R. Bamford, and K. Clark, "Clinical viral infections and multiple sclerosis," *Lancet*, vol. 1, no. 8441, pp. 1313–1315, 1985.

[13] P. B. Challoner, K. T. Smith, J. D. Parker, et al., "Plaque-associated expression of human herpesvirus 6 in multiple sclerosis," *Proceedings of the National Academy of Sciences of the United States of America*, vol. 92, no. 16, pp. 7440–7444, 1995.

[14] F. G. A. Moore and C. Wolfson, "Human herpes virus 6 and multiple sclerosis," *Acta Neurologica Scandinavica*, vol. 106, no. 2, pp. 63–83, 2002.

[15] S. S. Soldan, T. P. Leist, K. N. Juhng, H. F. McFarland, and S. Jacobson, "Increased lymphoproliferative response to human herpesvirus type 6A variant in multiple sclerosis patients," *Annals of Neurology*, vol. 47, no. 3, pp. 306–313, 2000.

[16] K.-P. Wandinger, W. Jabs, A. Siekhaus, et al., "Association between clinical disease activity and Epstein-Barr virus reactivation in MS," *Neurology*, vol. 55, no. 2, pp. 178–184, 2000.

[17] C. N. Martyn, M. Cruddas, and D. A. S. Compston, "Symptomatic Epstein-Barr virus infection and multiple sclerosis," *Journal of Neurology Neurosurgery and Psychiatry*, vol. 56, no. 2, pp. 167–168, 1993.

[18] M. C. Dal Canto, B. S. Kim, S. D. Miller, and R. W. Melvold, "Theiler's murine encephalomyelitis virus (TMEV)-induced demyelination: a model for human multiple sclerosis," *Methods*, vol. 10, no. 3, pp. 453–461, 1996.

[19] E. L. Oleszak, J. R. Chang, H. Friedman, C. D. Katsetos, and C. D. Platsoucas, "Theiler's virus infection: a model for multiple sclerosis," *Clinical Microbiology Reviews*, vol. 17, no. 1, pp. 174–207, 2004.

[20] J. J. Houtman and J. O. Fleming, "Pathogenesis of mouse hepatitis virus-induced demyelination," *Journal of NeuroVirology*, vol. 2, no. 6, pp. 361–376, 1996.

[21] E. Lavi, D. H. Gilden, and Z. Wroblewska, "Experimental demyelination produced by the A59 strain of mouse hepatitis virus," *Neurology*, vol. 34, no. 5, pp. 597–603, 1984.

[22] S. A. Stohlman and L. P. Weiner, "Chronic central nervous system demyelination in mice after JHM virus infection," *Neurology*, vol. 31, no. 1, pp. 38–44, 1981.

[23] L. P. Weiner, "Pathogenesis of demyelination induced by a mouse hepatitis," *Archives of Neurology*, vol. 28, no. 5, pp. 298–303, 1973.

[24] E. Lavi, D. H. Gilden, M. K. Highkin, and S. R. Weiss, "Persistence of mouse hepatitis virus A59 RNA in a slow virus demyelinating infection in mice as detected by in situ hybridization," *Journal of Virology*, vol. 51, no. 2, pp. 563–566, 1984.

[25] S. Perlman, G. Jacobson, A. L. Olson, and A. Afifi, "Identification of the spinal cord as a major site of persistence during chronic infection with a murine coronavirus," *Virology*, vol. 175, no. 2, pp. 418–426, 1990.

[26] J. L. Gombold and S. R. Weiss, "Mouse Hepatitis Virus A59 increases steady-state levels of MHC mRNAs in primary glial cell cultures and in the murine Central Nervous System," *Microbial Pathogenesis*, vol. 13, no. 6, pp. 493–505, 1992.

[27] E. Lavi, A. Suzumura, L. A. Lampson, et al., "Expression of MHC class I genes in mouse hepatitis virus (MHV-A59) infection and in multiple sclerosis," *Advances in Experimental Medicine and Biology*, vol. 218, pp. 219–222, 1987.

[28] E. Lavi, A. Suzumura, E. M. Murray, D. H. Silberberg, and S. R. Weiss, "Induction of MHC class I antigens on glial cells is dependent on persistent mouse hepatitis virus infection," *Journal of Neuroimmunology*, vol. 22, no. 2, pp. 107–111, 1989.

[29] A. Suzumura, E. Lavi, S. R. Weiss, and D. H. Silberberg, "Coronavirus infection induces H-2 antigen expression on oligodendrocytes and astrocytes," *Science*, vol. 232, no. 4753, pp. 991–993, 1986.

[30] A. Suzumura, E. Lavi, S. Bhat, D. Murasko, S. R. Weiss, and D. H. Silberberg, "Induction of glial cell MHC antigen expression in neurotropic coronavirus infections. Characterization of the H-2-inducing soluble factor elaborated by infected brain cells," *Journal of Immunology*, vol. 140, no. 6, pp. 2068–2072, 1988.

[31] A. I. Kaplin, C. Krishnan, D. M. Deshpande, C. A. Pardo, and D. A. Kerr, "Diagnosis and management of acute myelopathies," *Neurologist*, vol. 11, no. 1, pp. 2–18, 2005.

[32] I. J. Koralnik, "New insights into progressive multifocal leukoencephalopathy," *Current Opinion in Neurology*, vol. 17, no. 3, pp. 365–370, 2004.

[33] M. C. Dal Canto and S. G. Rabinowitz, "Experimental models of virus-induced demyelination of the central nervous system," *Annals of Neurology*, vol. 11, no. 2, pp. 109–127, 1982.

[34] S. D. Miller, C. L. Vanderlugt, W. S. Begolka, et al., "Persistent infection with Theiler's virus leads to CNS autoimmunity via epitope spreading," *Nature Medicine*, vol. 3, no. 10, pp. 1133–1136, 1997.

[35] M. Rodriguez and S. Sriram, "Successful therapy of Theiler's virus-induced demyelination (DA strain) with monoclonal anti-Lyt-2 antibody," *Journal of Immunology*, vol. 140, no. 9, pp. 2950–2955, 1988.

[36] M. Yamada, A. Zurbriggen, and R. S. Fujinami, "Monoclonal antibody to Theiler's murine encephalomyelitis virus defines a determinant on myelin and oligodendrocytes, and augments demyelination in experimental allergic encephalomyelitis," *Journal of Experimental Medicine*, vol. 171, no. 6, pp. 1893–1907, 1990.

[37] I. Tsunoda, Y. Iwasaki, H. Terunuma, K. Sako, and Y. Ohara, "A comparative study of acute and chronic diseases induced by two subgroups of Theiler's murine encephalomyelitis virus," *Acta Neuropathologica*, vol. 91, no. 6, pp. 595–602, 1996.

[38] C. P. Rossi, M. Delcroix, I. Huitinga, et al., "Role of macrophages during Theiler's virus infection," *Journal of Virology*, vol. 71, no. 4, pp. 3336–3340, 1997.

[39] J. S. Haring, L. L. Pewe, and S. Perlman, "Bystander CD8 T cell-mediated demyelination after viral infection of the central nervous system," *Journal of Immunology*, vol. 169, no. 3, pp. 1550–1555, 2002.

[40] F.-I. Wang, S. A. Stohlman, and J. O. Fleming, "Demyelination induced by murine hepatitis virus JHM strian (MHV-4) is immunologically mediated," *Journal of Neuroimmunology*, vol. 30, no. 1, pp. 31–41, 1990.

[41] G. F. Wu, A. A. Dandekar, L. Pewe, and S. Perlman, "CD4 and CD8 T cells have redundant but not identical roles in virus- induced demyelination," *Journal of Immunology*, vol. 165, no. 4, pp. 2278–2286, 2000.

[42] A. E. Matthews, E. Lavi, S. R. Weiss, and Y. Paterson, "Neither B cells nor T cells are required for CNS demyelination in mice persistently infected with MHV-A59," *Journal of NeuroVirology*, vol. 8, no. 3, pp. 257–264, 2002.

[43] R. M. Sutherland, M.-M. Chua, E. Lavi, S. R. Weiss, and Y. Paterson, "$CD4^+$ and $CD8^+$ T cells are not major effectors of mouse hepatitis virus A59-induced demyelinating disease," *Journal of NeuroVirology*, vol. 3, no. 3, pp. 225–228, 1997.

[44] K. McIntosh, R. K. Chao, H. E. Krause, R. Wasil, H. E. Mocega, and M. A. Mufson, "Coronavirus infection in acute lower respiratory tract disease of infants," *The Journal of Infectious Diseases*, vol. 130, p. 502, 1974.

[45] M. M. Lai and D. Cavanagh, "The molecular biology of coronaviruses," *Advances in Virus Research*, vol. 48, pp. 1–100, 1997.

[46] J. M. Gonzalez, P. Gomez-Puertas, D. Cavanagh, A. E. Gorbalenya, and L. Enjuanes, "A comparative sequence analysis to revise the current taxonomy of the family Coronaviridae," *Archives of Virology*, vol. 148, no. 11, pp. 2207–2235, 2003.

[47] J. D. Sarma, L. Fu, S. T. Hingley, and E. Lavi, "Mouse hepatitis virus type-2 infection in mice: an experimental model system of acute meningitis and hepatitis," *Experimental and Molecular Pathology*, vol. 71, no. 1, pp. 1–12, 2001.

[48] J. K. Fazakerley and M. J. Buchmeier, "Pathogenesis of virus-induced demyelination," *Advances in Virus Research*, vol. 42, pp. 249–324, 1993.

[49] M. Tardieu, O. Boespflug, and T. Barbe, "Selective tropism of a neurotropic coronavirus for ependymal cells, neurons, and meningeal cells," *Journal of Virology*, vol. 60, no. 2, pp. 574–582, 1986.

[50] S. Cheley, R. Anderson, M. J. Cupples, E. C. M. Lee Chana, and V. L. Morris, "Intracellular murine hepatitis virus-specific RNAs contain common sequences," *Virology*, vol. 112, no. 2, pp. 596–604, 1981.

[51] H. Vennema, G.-J. Godeke, J. W. A. Rossen, et al., "Nucleocapsid-independent assembly of coronavirus-like particles by co-expression of viral envelope protein genes," *EMBO Journal*, vol. 15, no. 8, pp. 2020–2028, 1996.

[52] F. Fischer, D. Peng, S. T. Hingley, S. R. Weiss, and P. S. Masters, "The internal open reading frame within the nucleocapsid gene of mouse hepatitis virus encodes a structural protein that is not essential for viral replication," *Journal of Virology*, vol. 71, no. 2, pp. 996–1003, 1997.

[53] D. A. Brian and R. S. Baric, "Coronavirus genome structure and replication," *Current Topics in Microbiology and Immunology*, vol. 287, pp. 1–30, 2005.

[54] A. E. Gorbalenya, E. V. Koonin, and M. M.-C. Lai, "Putative papain-related thiol proteases of positive-strand RNA viruses. Identification of rubi- and aphthovirus proteases and delineation of a novel conserved domain associated with proteases of rubi, α- and coronaviruses," *FEBS Letters*, vol. 288, no. 1-2, pp. 201–205, 1991.

[55] W. Spaan, D. Cavanagh, and M. C. Horzinek, "Coronaviruses: structure and genome expression," *Journal of General Virology*, vol. 69, no. 12, pp. 2939–2952, 1988.

[56] G. S. Dveksler, C. W. Dieffenbach, C. B. Cardellichio, et al., "Several members of the mouse carcinoembryonic antigen-related glycoprotein family are functional receptors for the coronavirus mouse hepatitis virus-A59," *Journal of Virology*, vol. 67, no. 1, pp. 1–8, 1993.

[57] E. Prentice and M. R. Denison, "The cell biology of coronavirus infection," *Advances in Experimental Medicine and Biology*, vol. 494, pp. 609–614, 2001.

[58] K. L. Tyler, D. A. McPhee, and B. N. Fields, "Distinct pathways of viral spread in the host determined by reovirus S1 gene segment," *Science*, vol. 233, no. 4765, pp. 770–774, 1986.

[59] E. V. Agapov, I. Frolov, B. D. Lindenbach, B. M. Pragai, S. Schlesinger, and C. M. Rice, "Noncytopathic sindbis virus RNA vectors for heterologous gene expression," *Proceedings of the National Academy of Sciences of the United States of America*, vol. 95, no. 22, pp. 12989–12994, 1998.

[60] J.-C. Boyer and A.-L. Haenni, "Infectious transcripts and cDNA clones of RNA viruses," *Virology*, vol. 198, no. 1, pp. 415–426, 1994.

[61] S. Makino, J. G. Keck, S. A. Stohlman, and M. M. C. Lai, "High-frequency RNA recombination of murine coronaviruses," *Journal of Virology*, vol. 57, no. 3, pp. 729–737, 1986.

[62] C. A. Koetzner, M. M. Parker, C. S. Ricard, L. S. Sturman, and P. S. Masters, "Repair and mutagenesis of the genome of a deletion mutant of the coronavirus mouse hepatitis virus by targeted RNA recombination," *Journal of Virology*, vol. 66, no. 4, pp. 1841–1848, 1992.

[63] L. Kuo, G.-J. Godeke, M. J. B. Raamsman, P. S. Masters, and P. J. M. Rottier, "Retargeting of coronavirus by substitution of the spike glycoprotein ectodomain: crossing the host cell species barrier," *Journal of Virology*, vol. 74, no. 3, pp. 1393–1406, 2000.

[64] P. S. Masters, "Reverse genetics of the largest RNA viruses," *Advances in Virus Research*, vol. 53, pp. 245–264, 1999.

[65] B. Yount, M. R. Denison, S. R. Weiss, and R. S. Baric, "Systematic assembly of a full-length infectious cDNA of mouse hepatitis virus strain A59," *Journal of Virology*, vol. 76, no. 21, pp. 11065–11078, 2002.

[66] E. F. Donaldson, B. Yount, A. C. Sims, S. Burkett, R. J. Pickles, and R. S. Baric, "Systematic assembly of a full-length infectious clone of human coronavirus NL63," *Journal of Virology*, vol. 82, no. 23, pp. 11948–11957, 2008.

[67] J. M. González, Z. Pénzes, F. Almazán, E. Calvo, and L. Enjuanes, "Stabilization of a full-length infectious cDNA clone of transmissible gastroenteritis coronavirus by insertion of an intron," *Journal of Virology*, vol. 76, no. 9, pp. 4655–4661, 2002.

[68] B. Yount, K. M. Curtis, E. A. Fritz, et al., "Reverse genetics with a full-length infectious cDNA of severe acute respiratory syndrome coronavirus," *Proceedings of the National Academy of Sciences of the United States of America*, vol. 100, no. 22, pp. 12995–13000, 2003.

[69] R. S. Baric and A. C. Sims, "Development of mouse hepatitis virus and SARS-CoV infectious cDNA constructs," *Current Topics in Microbiology and Immunology*, vol. 287, pp. 229–252, 2005.

[70] E. Lavi, P. S. Fishman, M. K. Highkin, and S. R. Weiss, "Limbic encephalitis after inhalation of a murine coronavirus," *Laboratory Investigation*, vol. 58, no. 1, pp. 31–36, 1988.

[71] M. Tardieu, A. Goffinet, G. Harmant-van Rijckevorsel, and G. Lyon, "Ependymitis, leukoencephalitis, hydrocephalus, and thrombotic vasculitis following chronic infection by mouse hepatitis virus 3 (MHV 3)," *Acta Neuropathologica*, vol. 58, no. 3, pp. 168–176, 1982.

[72] A. A. Dandekar, G. F. Wu, L. Pewe, and S. Perlman, "Axonal damage is T cell mediated and occurs concomitantly with demyelination in mice infected with a neurotropic coronavirus," *Journal of Virology*, vol. 75, no. 13, pp. 6115–6120, 2001.

[73] J. Das Sarma, L. C. Kenyon, S. T. Hingley, and K. S. Shindler, "Mechanisms of primary axonal damage in a viral model of multiple sclerosis," *Journal of Neuroscience*, vol. 29, no. 33, pp. 10272–10280, 2009.

[74] M. A. Sussman, R. A. Shubin, S. Kyuwa, and S. A. Stohlman, "T-cell mediated clearance of mouse hepatitis virus strain JHM from the central nervous system," *Journal of Virology*, vol. 63, no. 7, pp. 3051–3056, 1989.

[75] S. A. Stohlman, C. C. Bergmann, R. C. Van der Veen, and D. R. Hinton, "Mouse hepatitis virus-specific cytotoxic T lymphocytes protect from lethal infection without eliminating virus from the central nervous system," *Journal of Virology*, vol. 69, no. 2, pp. 684–694, 1995.

[76] S. A. Stohlman, C. C. Bergmann, M. T. Lin, D. J. Cua, and D. R. Hinton, "CTL effector function within the central nervous system requires $CD4^+$ T cells," *Journal of Immunology*, vol. 160, no. 6, pp. 2896–2904, 1998.

[77] J. O. Fleming, F.-I. Wang, M. D. Trousdale, D. R. Hinton, and S. A. Stohlman, "Interaction of immune and central nervous systems: contribution of anti- viral Thy-1+ cells to demyelination induced by coronavirus JHM," *Regional Immunology*, vol. 5, no. 1, pp. 37–43, 1993.

[78] J. J. Houtman and J. O. Fleming, "Dissociation of demyelination and viral clearance in congenitally immunodeficient mice infected with murine coronavirus JHM," *Journal of NeuroVirology*, vol. 2, no. 2, pp. 101–110, 1996.

[79] A. A. Dandekar and S. Perlman, "Virus-induced demyelination in nude mice is mediated by $\gamma\delta$ T cells," *American Journal of Pathology*, vol. 161, no. 4, pp. 1255–1263, 2002.

[80] R. L. Knobler, P. W. Lampert, and M. B. A. Oldstone, "Virus persistence and recurring demyelination produced by a temperature-sensitive mutant of MHV-4," *Nature*, vol. 298, no. 5871, pp. 279–280, 1982.

[81] J. Das Sarma, L. Fu, J. C. Tsai, S. R. Weiss, and E. Lavi, "Demyelination determinants map to the spike glycoprotein gene of coronavirus mouse hepatitis virus," *Journal of Virology*, vol. 74, no. 19, pp. 9206–9213, 2000.

[82] J. Das Sarma, L. Fu, S. T. Hingley, M. M. C. Lai, and E. Lavi, "Sequence analysis of the S gene of recombinant MHV-2/A59 coronaviruses reveals three candidate mutations associated with demyelination and hepatitis," *Journal of NeuroVirology*, vol. 7, no. 5, pp. 432–436, 2001.

[83] M. V. Haspel, P. W. Lampert, and M. B. A. Oldstone, "Temperature-sensitive mutants of mouse hepatitis virus produce a high incidence of demyelination," *Proceedings of the National Academy of Sciences of the United States of America*, vol. 75, no. 8, pp. 4033–4036, 1978.

[84] R. L. Knobler, M. V. Haspel, and M. B. A. Oldstone, "Mouse hepatitis virus type 4 (JHM strain)-induced fatal central nervous system disease. I. Genetic control and the murine neuron as the susceptible site of disease," *Journal of Experimental Medicine*, vol. 153, no. 4, pp. 832–843, 1981.

[85] Y. Li, L. Fu, D. M. Gonzales, and E. Lavi, "Coronavirus neurovirulence correlates with the ability of the virus to induce proinflammatory cytokine signals from astrocytes and microglia," *Journal of Virology*, vol. 78, no. 7, pp. 3398–3406, 2004.

[86] B. D. Pearce, M. V. Hobbs, T. S. McGraw, and M. J. Buchmeier, "Cytokine induction during T-cell-mediated clearance of mouse hepatitis virus from neurons in vivo," *Journal of Virology*, vol. 68, no. 9, pp. 5483–5495, 1994.

[87] B. Parra, D. R. Hinton, M. T. Lin, D. J. Cua, and S. A. Stohlman, "Kinetics of cytokine mRNA expression in the central nervous system following lethal and nonlethal coronavirus-induced acute encephalomyelitis," *Virology*, vol. 233, no. 2, pp. 260–270, 1997.

[88] M. J. Buchmeier and T. E. Lane, "Viral-induced neurodegenerative disease," *Current Opinion in Microbiology*, vol. 2, no. 4, pp. 398–402, 1999.

[89] N. Sun, D. Grzybicki, R. F. Castro, S. Murphy, and S. Perlman, "Activation of astrocytes in the spinal cord of mice chronically infected with a neutropic coronavirus," *Virology*, vol. 213, no. 2, pp. 482–493, 1995.

[90] J. G. Keck, L. H. Soe, S. Makino, S. A. Stohlman, and M. M. C. Lai, "RNA recombination of murine coronaviruses: recombination between fusion-positive mouse hepatitis virus A59 and fusion-negative mouse hepatitis virus 2," *Journal of Virology*, vol. 62, no. 6, pp. 1989–1998, 1988.

[91] R. L. Knobler, M. Dubois-Dalcq, M. V. Haspel, A. P. Claysmith, P. W. Lampert, and M. B. Oldstone, "Selective localization of wild type and mutant mouse hepatitis virus (JHM strain) antigens in CNS tissue by fluorescence, light and electron microscopy," *Journal of Neuroimmunology*, vol. 1, p. 81, 1981.

[92] L. P. Weiner, R. T. Johnson, and R. M. Herndon, "Viral infections and demyelinating diseases," *The New England Journal of Medicine*, vol. 288, no. 21, pp. 1103–1110, 1973.

[93] Y. K. Yamada, K. Takimoto, M. Yabe, and F. Taguchi, "Acquired fusion activity of a murine coronavirus MHV-2 variant with mutations in the proteolytic cleavage site and the signal sequence of the S protein," *Virology*, vol. 227, no. 1, pp. 215–219, 1997.

[94] K. S. Shindler, L. C. Kenyon, M. Dutt, S. T. Hingley, and J. Das Sarma, "Experimental optic neuritis induced by a demyelinating strain of mouse hepatitis virus," *Journal of Virology*, vol. 82, no. 17, pp. 8882–8886, 2008.

[95] B. Kornek, M. K. Storch, R. Weissert, et al., "Multiple sclerosis and chronic autoimmune encephalomyelitis: a comparative quantitative study of axonal injury in active, inactive, and remyelinated lesions," *American Journal of Pathology*, vol. 157, no. 1, pp. 267–276, 2000.

[96] K. S. Shindler, Y. Guan, E. Ventura, J. Bennett, and A. Rostami, "Retinal ganglion cell loss induced by acute optic neuritis in a relapsing model of multiple sclerosis," *Multiple Sclerosis*, vol. 12, no. 5, pp. 526–532, 2006.

[97] H. Shao, Z. Huang, S. L. Sun, H. J. Kaplan, and D. Sun, "Myelin/oligodendrocyte glycoprotein-specific T-cells induce severe optic neuritis in the C57B1/6 mouse," *Investigative Ophthalmology and Visual Science*, vol. 45, no. 11, pp. 4060–4065, 2004.

[98] K. S. Shindler, E. Ventura, T. S. Rex, P. Elliott, and A. Rostami, "SIRT1 activation confers neuroprotection in experimental optic neuritis," *Investigative Ophthalmology and Visual Science*, vol. 48, no. 8, pp. 3602–3609, 2007.

[99] K. S. Shindler, E. Ventura, M. Dutt, and A. Rostami, "Inflammatory demyelination induces axonal injury and retinal ganglion cell apoptosis in experimental optic neuritis," *Experimental Eye Research*, vol. 87, no. 3, pp. 208–213, 2008.

[100] J. H. Noseworthy, C. Lucchinetti, M. Rodriguez, and B. G. Weinshenker, "Multiple sclerosis," *The New England Journal of Medicine*, vol. 343, no. 13, pp. 938–952, 2000.

[101] M. K. Guyton, E. A. Sribnick, S. K. Ray, and N. L. Banik, "A role for calpain in optic neuritis," *Annals of the New York Academy of Sciences*, vol. 1053, pp. 48–54, 2005.

[102] X. Qi, A. S. Lewin, L. Sun, W. W. Hauswirth, and J. Guy, "Suppression of mitochondrial oxidative stress provides

long-term neuroprotection in experimental optic neuritis," *Investigative Ophthalmology and Visual Science*, vol. 48, no. 2, pp. 681–691, 2007.

[103] M. B. Sättler, D. Merkler, K. Maier, et al., "Neuroprotective effects and intracellular signaling pathways of erythropoietin in a rat model of multiple sclerosis," *Cell Death and Differentiation*, vol. 11, supplement 2, pp. S181–S192, 2004.

[104] M. Hobom, M. K. Storch, R. Weissert, et al., "Mechanisms and time course of neuronal degeneration in experimental autoimmune encephalomyelitis," *Brain Pathology*, vol. 14, no. 2, pp. 148–157, 2004.

[105] T. M. Gallagher and M. J. Buchmeier, "Coronavirus spike proteins in viral entry and pathogenesis," *Virology*, vol. 279, no. 2, pp. 371–374, 2001.

[106] S. T. Hingley, J. L. Gombold, E. Lavi, and S. R. Weiss, "MHV-A59 fusion mutants are attenuated and display altered hepatotropism," *Virology*, vol. 200, no. 1, pp. 1–10, 1994.

[107] J. J. Phillips, M. M. Chua, E. Lavi, and S. R. Weiss, "Pathogenesis of chimeric MHV4/MHV-A59 recombinant viruses: the murine coronavirus spike protein is a major determinant of neurovirulence," *Journal of Virology*, vol. 73, no. 9, pp. 7752–7760, 1999.

[108] J. J. Phillips, M. M. Chua, G. F. Rall, and S. R. Weiss, "Murine coronavirus spike glycoprotein mediates degree of viral spread, inflammation, and virus-induced immunopathology in the central nervous system," *Virology*, vol. 301, no. 1, pp. 109–120, 2002.

[109] J. J. Phillips and S. R. Weiss, "MHV neuropathogenesis: the study of chimeric S genes and mutations in the hypervariable region," *Advances in Experimental Medicine and Biology*, vol. 494, pp. 115–119, 2001.

[110] S. Navas, S.-H. Seo, M. M. Chua, et al., "Murine coronavirus spike protein determines the ability of the virus to replicate in the liver and cause hepatitis," *Journal of Virology*, vol. 75, no. 5, pp. 2452–2457, 2001.

[111] I. Leparc-Goffart, S. T. Hingley, M. M. Chua, J. Phillips, E. Lavi, and S. R. Weiss, "Targeted recombination within the spike gene of murine coronavirus mouse hepatitis virus-A59: Q159 is a determinant of hepatotropism," *Journal of Virology*, vol. 72, no. 12, pp. 9628–9636, 1998.

[112] J. C. Tsai, L. De Groot, J. D. Pinon, et al., "Amino acid substitutions within the heptad repeat domain 1 of murine coronavirus spike protein restrict viral antigen spread in the central nervous system," *Virology*, vol. 312, no. 2, pp. 369–380, 2003.

[113] F. Fischer, C. F. Stegen, C. A. Koetzner, and P. S. Masters, "Analysis of a recombinant mouse hepatitis virus expressing a foreign gene reveals a novel aspect of coronavirus transcription," *Journal of Virology*, vol. 71, no. 7, pp. 5148–5160, 1997.

[114] J. Das Sarma, E. Scheen, S.-H. Seo, M. Koval, and S. R. Weiss, "Enhanced green fluorescent protein expression may be used to monitor murine coronavirus spread in vitro and in the mouse central nervous system," *Journal of NeuroVirology*, vol. 8, no. 5, pp. 381–391, 2002.

[115] E. Ontiveros, L. Kuo, P. S. Masters, and S. Perlman, "Inactivation of expression of gene 4 of mouse hepatitis virus strain JHM does not affect virulence in the murine CNS," *Virology*, vol. 289, no. 2, pp. 230–238, 2001.

[116] J. Das Sarma, K. Iacono, L. Gard, et al., "Demyelinating and nondemyelinating strains of mouse hepatitis virus differ in their neural cell tropism," *Journal of Virology*, vol. 82, no. 11, pp. 5519–5526, 2008.

[117] P. De Camilli, P. E. Miller, F. Navone, W. E. Theurkauf, and R. B. Vallee, "Distribution of microtubule-associated protein 2 in the nervous system of the rat studied by immunofluorescence," *Neuroscience*, vol. 11, no. 4, pp. 819–846, 1984.

[118] A. Gadea, S. Schinelli, and V. Gallo, "Endothelin-1 regulates astrocyte proliferation and reactive gliosis via a JNK/c-Jun signaling pathway," *Journal of Neuroscience*, vol. 28, no. 10, pp. 2394–2408, 2008.

[119] J. M. M. Pasick, K. Kalicharran, and S. Dales, "Distribution and trafficking of JHM coronavirus structural proteins and virions in primary neurons and the OBL-21 neuronal cell line," *Journal of Virology*, vol. 68, no. 5, pp. 2915–2928, 1994.

[120] H. L. Weiner, M. L. Powers, and B. N. Fields, "Absolute linkage of virulence and central nervous system cell tropism of reoviruses to viral hemagglutinin," *Journal of Infectious Diseases*, vol. 141, no. 5, pp. 609–616, 1980.

[121] L. J. Zoecklein, K. D. Pavelko, J. Gamez, et al., "Direct comparison of demyelinating disease induced by the Daniel's strain and BeAn strain of Theiler's murine encephalomyelitis virus," *Brain Pathology*, vol. 13, no. 3, pp. 291–308, 2003.

[122] D. Moskophidis, M. Battegay, M. Van den Broek, E. Laine, U. Hoffmann-Rohrer, and R. M. Zinkernagel, "Role of virus and host variables in virus persistence or immunopathological disease caused by a non-cytolytic virus," *Journal of General Virology*, vol. 76, no. 2, pp. 381–391, 1995.

[123] D. Wodarz and D. C. Krakauer, "Defining CTL-induced pathology: implications for HIV," *Virology*, vol. 274, no. 1, pp. 94–104, 2000.

[124] K. C. MacNamara, M. M. Chua, P. T. Nelson, H. Shen, and S. R. Weiss, "Increased epitope-specific $CD8^+$ T cells prevent murine coronavirus spread to the spinal cord and subsequent demyelination," *Journal of Virology*, vol. 79, no. 6, pp. 3370–3381, 2005.

[125] L. W. Enquist, P. J. Husak, B. W. Banfield, and G. A. Smith, "Infection and spread of alphaherpesviruses in the nervous system," *Advances in Virus Research*, vol. 51, pp. 237–347, 1998.

[126] L. W. Enquist, M. J. Tomishima, S. Gross, and G. A. Smith, "Directional spread of an α-herpesvirus in the nervous system," *Veterinary Microbiology*, vol. 86, no. 1-2, pp. 5–16, 2002.

[127] J.-P. Roussarie, C. Ruffie, J. M. Edgar, I. Griffiths, and M. Brahic, "Axon myelin transfer of a non-enveloped virus," *PLoS ONE*, vol. 2, no. 12, article e1331, 2007.

[128] E. Lavi, A. Suzumura, M. Hirayama, et al., "Coronavirus mouse hepatitis virus (MHV)-A59 causes a persistent, productive infection in primary glial cell cultures," *Microbial Pathogenesis*, vol. 3, no. 2, pp. 79–86, 1987.

[129] K. Kalicharran and S. Dales, "The murine coronavirus as a model of trafficking and assembly of viral proteins in neural tissue," *Trends in Microbiology*, vol. 4, no. 7, pp. 264–269, 1996.

[130] K. Kalicharran, D. Mohandas, G. Wilson, and S. Dales, "Regulation of the initiation of coronavirus JHM infection in primary oligodendrocytes and L-2 fibroblasts," *Virology*, vol. 225, no. 1, pp. 33–43, 1996.

[131] E. O. Major, K. Amemiya, C. S. Tornatore, S. A. Houff, and J. R. Berger, "Pathogenesis and molecular biology of progressive multifocal leukoencephalopathy, the JC virus-induced demyelinating disease of the human brain," *Clinical Microbiology Reviews*, vol. 5, no. 1, pp. 49–73, 1992.

[132] S. M. Richardson-Burns, B. K. Kleinschmidt-DeMasters, R. L. DeBiasi, and K. L. Tyler, "Progressive multifocal leukoencephalopathy and apoptosis of infected oligodendrocytes in the central nervous system of patients with and without AIDS," *Archives of Neurology*, vol. 59, no. 12, pp. 1930–1936, 2002.

[133] D. S. Chen, M. Asanaka, F. S. Chen, J. E. Shively, and M. M. C. Lai, "Human carcinoembryonic antigen and biliary glycoprotein can serve as mouse hepatitis virus receptors," *Journal of Virology*, vol. 71, no. 2, pp. 1688–1691, 1997.

[134] K. Tan, B. D. Zelus, R. Meijers, et al., "Crystal structure of murine sCEACAM1a[1,4]: a coronavirus receptor in the CEA family," *EMBO Journal*, vol. 21, no. 9, pp. 2076–2086, 2002.

[135] T. M. Gallagher, M. J. Buchmeier, and S. Perlman, "Cell receptor-independent infection by a neurotropic murine coronavirus," *Virology*, vol. 191, no. 1, pp. 517–522, 1992.

[136] M. F. Frana, J. N. Behnke, L. S. Sturman, and K. V. Holmes, "Proteolytic cleavage of the E2 glycoprotein of murine coronavirus: host-dependent differences in proteolytic cleavage and cell fusion," *Journal of Virology*, vol. 56, no. 3, pp. 912–920, 1985.

[137] H. Kubo, Y. K. Yamada, and F. Taguchi, "Localization of neutralizing epitopes and the receptor-binding site within the amino-terminal 330 amino acids of the murine coronavirus spike protein," *Journal of Virology*, vol. 68, no. 9, pp. 5403–5410, 1994.

[138] T. M. Gallagher and M. J. Buchmeier, "Coronavirus spike proteins in viral entry and pathogenesis," *Virology*, vol. 279, no. 2, pp. 371–374, 2001.

[139] S. Matsuyama and F. Taguchi, "Receptor-induced conformational changes of murine coronavirus spike protein," *Journal of Virology*, vol. 76, no. 23, pp. 11819–11826, 2002.

[140] B. D. Zelus, J. H. Schickli, D. M. Blau, S. R. Weiss, and K. V. Holmes, "Conformational changes in the spike glycoprotein of murine coronavirus are induced at 37°C either by soluble murine CEACAM1 receptors or by pH8," *Journal of Virology*, vol. 77, no. 2, pp. 830–840, 2003.

[141] Z. Luo and S. R. Weiss, "Roles in cell-to-cell fusion of two conserved hydrophobic regions in the murine coronavirus spike protein," *Virology*, vol. 244, no. 2, pp. 483–494, 1998.

[142] C. A. M. de Haan, P. S. Masters, X. Shen, S. Weiss, and P. J. M. Rottier, "The group-specific murine coronavirus genes are not essential, but their deletion, by reverse genetics, is attenuating in the natural host," *Virology*, vol. 296, no. 1, pp. 177–189, 2002.

[143] B. Charley and H. Laude, "Induction of alpha interferon by transmissible gastroenteritis coronavirus: role of transmembrane glycoprotein E1," *Journal of Virology*, vol. 62, no. 1, pp. 8–11, 1988.

[144] C. A. M. de Haan, M. de Wit, L. Kuo, et al., "O-glycosylation of the mouse hepatitis coronavirus membrane protein," *Virus Research*, vol. 82, no. 1-2, pp. 77–81, 2002.

[145] A. Hirano, A. H. Wang, A. F. Gombart, and T. C. Wong, "The matrix proteins of neurovirulent subacute sclerosing panencephalitis virus and its acute measles virus progenitor are functionally different," *Proceedings of the National Academy of Sciences of the United States of America*, vol. 89, no. 18, pp. 8745–8749, 1992.

[146] Q. Ning, M. Liu, P. Kongkham, et al., "The nucleocapsid protein of murine hepatitis virus type 3 induces transcription of the novel fgl2 prothrombinase gene," *Journal of Biological Chemistry*, vol. 274, no. 15, pp. 9930–9936, 1999.

[147] P. S. Masters, C. A. Koetzner, C. A. Kerr, and Y. Heo, "Optimization of targeted RNA recombination and mapping of a novel nucleocapsid gene mutation in the coronavirus mouse hepatitis virus," *Journal of Virology*, vol. 68, no. 1, pp. 328–337, 1994.

[148] S. R. Weiss, P. W. Zoltick, and J. L. Leibowitz, "The ns 4 gene of mouse hepatitis virus (MHV), strain A 59 contains two ORFs and thus differs from ns 4 of the JHM and S strains," *Archives of Virology*, vol. 129, no. 1–4, pp. 301–309, 1993.